Aus der Radiologischen Universitätsklinik Tübingen

Abteilung für Diagnostische und Interventionelle Radiologie

MRI-based assessment of pericardial fat between subjects with diabetes, prediabetes and healthy controls in the general population

Inaugural-Dissertation

zur Erlangung des Doktorgrades

der Medizin

der Medizinischen Fakultät

der Eberhard Karls Universität

zu Tübingen

vorgelegt von

Rado, geb. Heber, Sophia Désirée

2020

Dekan: Professor Dr. I. B. Autenrieth

1. Berichterstatter: Professor Dr. F. Bamberg

2. Berichterstatter: Professor Dr. B. Gallwitz

Tag der Disputation: 08.01.2020

Meiner Mutter Dr. med. Viktoria M. Heber, meinem Vater Dipl.-Ing. Hans K. Heber und meinem Ehemann Dr. med. Yaron Rado für Ihre Unterstützung und Liebe

Table of Contents

List of tables

List of figures

List of abbreviations

ADA: American Diabetes Association

AGE: advanced glycation end-product

BMI: body mass index

CAD: coronary artery disease

CI: confidence interval

CMR: cardiac magnetic resonance

COPD: chronic obstructive pulmonary disease

CT: computed tomography

CVRF: cardiovascular risk factors

EF: ejection fraction

FLASH: Fast Low Angle Shot

FOV: field of view

GAD: glutamic acid decarboxylase

HbA1c: hemoglobin A1c

HDL: high-density lipoprotein

ICC: intraclass correlation coefficient

IFG: impaired fasting glucose

IGT: impaired glucose tolerance

IQR: interquartile range

KORA: Kooperative Gesundheitsforschung in der Region Augsburg (Cooperative Health Research in the Region Augsburg)

LGE: late gadolinium enhancement

LDL: low-density lipoprotein

LV: left ventricle

LVCI: left ventricular concentricity index

MONICA: Monitoring Trends and Determinants in Cardiovascular Disease

MR: magnetic resonance

MRI: magnetic resonance imaging

OGTT: oral glucose tolerance test

PDFF: proton density fat fraction

PET: positron emission tomography

ROI: region of interest

RV: right ventricle

SAT: subcutaneous adipose tissue

SSFP: steady state free precession

TE: time of echo

TI: inversion time

TR: time of repetition

US: United States

VAT: visceral adipose tissue

VIBE: volume interpolated breath hold

WHO: World Health Organization

1. Introduction

1.1. Impaired glucose metabolism: a global issue

The body's inability to control its blood glucose levels adequately can be described as impaired glucose metabolism and, if certain criteria are fulfilled, as diabetes mellitus. This kind of metabolic disorder is becoming more and more prevalent in today's world; thus, placing a huge burden onto our economic and healthcare systems.

On a global level, *Ogurtsova et al* estimated that in 2015, 415 million people worldwide between the ages 20-79 years had diabetes and that the global health costs due to diabetes were 673 billion US (United States) dollars (Ogurtsova et al. 2017). Another study found that in 2015, the global expenditure for diabetes was about 1.31 trillion US dollars including indirect costs (Bommer et al. 2017).

A study from the US comparing data sets from 1988-1994 and 2011-2012 with regards to diabetes prevalence found an increase over time with a prevalence between 12-14% in 2011-2012 (Menke et al. 2015). Data from another US-based study conducted in 2016-2017 showed a prevalence of diagnosed diabetes of 9.7%. This study also revealed that type 2 diabetes is predominant in comparison to type 1 diabetes (Xu et al. 2018).

Data for Germany show that while the prevalence of diabetes did not vary significantly between 1997-1999 and 2008-2011, there was an increase in diagnosed diabetes seen (Heidemann et al. 2016). *Tamayo et al* found that the diabetes prevalence was 9.9% in 2010 upon age and gender standardization (Tamayo et al. 2016). A study investigating the prevalence of gestational diabetes (pregnancy-related diabetes) in Germany between 2014-2015 found a prevalence of 13.2% (Melchior et al. 2017). Regional differences within Germany have been detected with regards to impaired glucose metabolism (Stöckl et al. 2016).

An increase in the prevalence of diabetes and the associated healthcare costs is expected in the future. Globally, it is expected that about 642 million people will be affected by diabetes in 2040 which will certainly have an impact on the social and financial systems (Ogurtsova et al. 2017).

In the following, the state of impaired glucose metabolism and diabetes will be defined and classified, signs and symptoms will be discussed, complications will be outlined and diagnostic options given.

1.1.1. Definition and types of prediabetes and diabetes mellitus

Impaired glucose metabolism and diabetes mellitus (in the latter referred to as diabetes) are characterized by a malfunctioning control of blood glucose levels due to varying conditions. Today, we differentiate between diabetes, impaired glucose tolerance (IGT) and impaired fasting glucose (IFG). The World Health Organization (WHO) defines diabetes as fasting plasma glucose ≥7.0 mmol/l (126 mg/dl) or 2-hour plasma glucose after administration of an oral glucose tolerance test (OGTT) consisting of 75g oral glucose, ≥ 11.1 mmol/l (200 mg/dl). IGT is defined as fasting plasma glucose <7.0 mmol/l (126 mg/dl) and 2-hour plasma glucose ≥7.8 and <11.1 mmol/l (140-200 mg/dl). IFG is defined as fasting plasma glucose between 6.1 and 6.9 mmol/l (110-125 mg/dl) and 2-hour plasma glucose <7.8 mmol/l (140 mg/dl) (World Health Organization and International Diabetes Federation 2006). The American Diabetes Association (ADA) Expert Committee lowered the levels for defining IFG from 6.1 mmol/l (110 mg/dl) to 5.6 mmol/l (100 mg/dl) in 2003 (Genuth et al. 2003). IGT and IFG can be summarized as prediabetes. Normal glucose tolerance is characterized as the absence of either prediabetes or diabetes.

Pathological changes in the blood glucose metabolism can have different underlying conditions. According to the ADA, there are four subgroups (American Diabetes Association 2018):

The first subgroup is called **type 1 diabetes** and is considered an autoimmune condition. Autoantibodies against insulin, islet cells, glutamic acid decarboxylase (GAD) and tyrosinphosphatases destroy the pancreatic insulin-producing β-cells, thus leading to an absolute deficiency of insulin (American Diabetes Association 2014). Type 1 diabetes

can occur in conjunction with other autoimmune and also genetic disorders (Kota et al. 2012) and reveals itself mostly during childhood. An upward trend in incidence has been reported (Patterson et al. 2009). A special subgroup is called idiopathic type 1 diabetes which is characterized by impaired production of insulin without signs for autoimmune processes (American Diabetes Association 2010). In a study published in 2018, the prevalence of type 1 diabetes in adults in the US was 0.5% and amongst adults diagnosed with diabetes, type 1 diabetes was the underlying subgroup in 5.6% (Xu et al. 2018).

Type 2 diabetes is nowadays the predominant form of diagnosed diabetes (Xu et al. 2018). The condition can be described as insulin-resistance of the target tissues in combination with a relative insulin deficiency (American Diabetes Association 2014). Type 2 diabetes is commonly seen in combination with other components of the metabolic syndrome such as impaired lipid metabolism, elevated blood pressure and obesity (Lin et al. 2015).

The term prediabetes encompasses IGT and/or IFG and represents the precursor stage of diabetes. More than one out of three adults in the US suffer from prediabetes (Menke et al. 2015) and it is a credible and often underestimated disease state, with an approximate 74.0% lifetime risk of progressing to diabetes (Ligthart et al. 2016). *Wu et al* showed that progression from newly diagnosed prediabetes to type 2 diabetes was 30.3% in 3 years (Wu et al. 2017).

Gestational diabetes (pregnancy-related diabetes) is difficult to distinguish from preexisting type 1 or type 2 diabetes. Currently, gestational diabetes is defined as a first-time diagnosis of diabetes in the second or third trimester without signs for pre-existing diabetes (American Diabetes Association 2018).

Other etiologies include genetic defects in insulin production as well as action, endocrine conditions, disorders of the exocrine pancreas system, diabetes related to contact with chemicals or intake of drugs, infections and less common forms of immune-mediated diabetes that can also lead to impaired glucose metabolism (American Diabetes Association 2014, American Diabetes Association 2018).

1.1.2. Symptoms of impaired glucose metabolism

There are no specific symptoms indicating prediabetes status. It has been found that patients with prediabetes did not show reduction in health-related quality of life in comparison to subjects with newly diagnosed diabetes (Seppälä et al. 2013).

In subjects affected by diabetes, symptoms can develop in hyperglycemia (high blood glucose levels) or hypoglycemia (low blood glucose levels) and can range from subtle to life-threatening. Typical hyperglycemic symptoms are polyuria (increased urination) and polydipsia (increased thirst) but also unspecific symptoms such as weight-loss or polyphagia (increased appetite) (American Diabetes Association 2014). A life-threatening complication of uncontrolled diabetes is called ketoacidosis. This condition is more often seen in type 1 diabetes and presents with high blood glucose levels, metabolic acidosis, and elevated ketone levels. The typical presentation of ketoacidosis includes symptoms such as polyuria, polydipsia, weight loss, fatigue, dyspnea, and vomiting as reviewed by *Westerberg* in 2013 (Westerberg 2013). On the other side, hypoglycemia can also be life-threatening and can present with autonomous, neuroglycopenic as well as malaise symptoms (Deary et al. 1993).

1.1.3. Complications and comorbidities

Due to the development of advanced glycation end-products (AGE) in the bloodstream affecting vessel walls, impaired glucose metabolism can lead to micro- and macrovascular changes; thus, contributing to the global vascular risk. This metabolic disorder predominantly affects the cardiovascular, renal, and nervous system as well as the retina (Fowler 2008). Microvascular and macrovascular disease in type 2 diabetes are both independently associated with an adverse cardiovascular outcome. The combination of both carries the highest risk (Mohammedi et al. 2017). Interestingly, many of the complications associated with impaired glucose metabolism are statistically similar in subjects with prediabetes as compared to type 2 diabetes (Farrell and Moran 2014).

Furthermore, diabetes and its complications pose a substantial economic burden on healthcare systems worldwide. A study published in 2002 showed that the costs of complications in type 2 diabetes were calculated to an estimate of 47,240 US dollar per patient over a time span of 30 years with macrovascular disease being responsible for the majority of the total cost over the first 5 years (Caro et al. 2002). Multiple chronic comorbidities are often seen with the leading cluster consisting of high blood pressure, hyperlipidemia and adiposity (Lin et al. 2015). Subsequently, the rate of complications increases over time (Grimaldi et al. 2000).

Microvascular complications

Chronic kidney disease in diabetes, also known as diabetic nephropathy, is seen in about 20-40% of all diabetics (American Diabetes Association 2007). In a prospective cohort study conducted in Singapore by *Low et al*, 45% of subjects with type 2 diabetes developed chronic kidney disease with albuminuria as the most common first manifestation (Low et al. 2016). Hypertension has been found to be an independent risk factor for diabetic nephropathy (Bentata et al. 2015).

Diabetic retinopathy (damage of the retina due to diabetes) affected approximately 93 million people worldwide in 2010 and its main features of retinal neovascularization and macular edema are potentially vision-threatening (Yau et al. 2012). Today, we discriminate the proliferative and the non-proliferative subtypes. Polyol accumulation, AGE, oxidative damage, proteinkinase C and growth factors have all been described as contributing factors, as extensively reviewed by *Fong et al* (Fong et al. 2004). Risk factors for diabetic retinopathy are elevated blood glucose and blood pressure as well as dyslipidemia (Yau et al. 2012).

The term **diabetic neuropathy** describes nerve damage due to diabetes and summarizes entities such as diabetic mononeuropathy, peripheral neuropathy and autonomic neuropathy. Its detailed pathophysiology is unknown; however, oxidative stress, polyol accumulation and AGE are considered to play a role (Fowler 2008). According to the ADA, reduction in the perception of vibration as well as loss of pressure

sensation as assessed by a 10g monofilament can be seen as predictors for the development of foot ulcers (American Diabetes Association 2007). Risk factors for peripheral diabetic neuropathy include, besides others, uncontrolled blood glucose levels as well as body height and age (Adler et al. 1997).

Macrovascular complications

Macrovascular complications such as coronary artery disease (CAD), peripheral arterial disease or cerebrovascular disease and stroke are mostly due to processes leading to atherosclerosis (Fowler 2008). Diabetes is associated with a two to threefold risk of atherosclerotic diseases and affects women more strongly than men (Kannel and McGee 1979). Data indicate that diabetes has deteriorating effects on the cardiac function as well (Devereux et al. 2000).

Comorbidities

Elderly patients with diabetes show an increased risk for **dementia** (Xu et al. 2004). Also, subjects with type 2 diabetes appear to have a higher prevalence of **depression** (Ali et al. 2006). It has, however, also been discussed that depressive symptoms may lead to a higher risk of type 2 diabetes in women (Arroyo et al. 2004). Also, a higher risk of **hip fractures** is suggested in patients with diabetes and potential explanations have been extensively reviewed by *Starup-Linde et al* (Starup-Linde et al. 2017). Additionally, subjects with impaired glucose metabolism are more prone to **infections**, e.g. post-surgery (Chen et al. 2009).

As described earlier, type 2 diabetes is often associated with comorbidity clusters which include **obesity** (Lin et al. 2015). Fat distribution plays an important role since visceral adipose tissue (VAT) seems to have a stronger negative effect on cardiometabolic risk markers than subcutaneous adipose tissue (SAT) (Liu et al. 2010). Interestingly,

abdominal superficial subcutaneous adipose tissue seems to have advantageous effects in subjects with diabetes (Golan et al. 2012). Additionally, it has been shown that the relation of VAT to SAT, the so-called VAT/SAT ratio, can predict cardiovascular disease in subjects with diabetes (Fukuda et al. 2018). In elderly women, abdominal obesity as defined by employing the waist-to-hip ratio has emerged as a risk factor for the development of diabetes (Kaye et al. 1991). VAT has been shown to be responsible for disturbances in the lipid-lipoprotein profiles in women with impaired glucose tolerance (Lemieux et al. 2011).

1.1.4. Diagnostics

Blood glucose levels should ideally be measured in venous blood plasma samples, as soon as the sample is drawn. Besides measurement of fasting glucose levels, a 75g OGTT may be administered on patients with suspected impaired glucose metabolism (World Health Organization and International Diabetes Federation 2006, American Diabetes Association 2014). Testing of glycosylated haemoglobin A1 (HbA1c), reflecting average blood glucose levels of the last 2 to 3 months, has been described as acceptable by the ADA in their 2018 Standards of Care, but a standardized and certified method is recommended (American Diabetes Association 2018). Subjects at risk for diabetes should undergo screening for diabetes and prediabetes (American Diabetes Association 2018).

1.2. The fat compartments surrounding the heart

Adipocytes are cells that primarily store energy-equivalents in the form of triglycerides. Clusters of adipocytes are called adipose tissue which can naturally be found in multiple locations in the body. Excess body fat is being stored in so-called ectopic fat depots. While some of these fat depots interact more locally with other surrounding cells and organs, others have systemic effects (Britton and Fox 2011). Examples for ectopic fat depots include VAT, pericardial fat, or hepatic fat (Britton and Fox 2011).

There is scientific evidence that ectopic fat depots, specifically VAT and epicardial fat are associated with cardiometabolic disease (Fox et al. 2007, Mahabadi et al. 2009).

In the following, the anatomy, physiology and pathophysiology of the fat depots surrounding the heart will be reviewed with a special emphasis on epicardial fat.

1.2.1. Anatomy and description of the pericardial fat depots

The heart is surrounded by different fat compartments. **Pericardial fat** can be seen as an umbrella term for the two distinct fat compartments **epicardial and paracardial fat** (Bertaso et al. 2013, Sacks and Fain 2007). Existing literature is highly inconsistent in the nomenclature of the fat compartment anatomy. Figure 1 outlines the localization of the different fat compartments as they will be referred to in the following study.

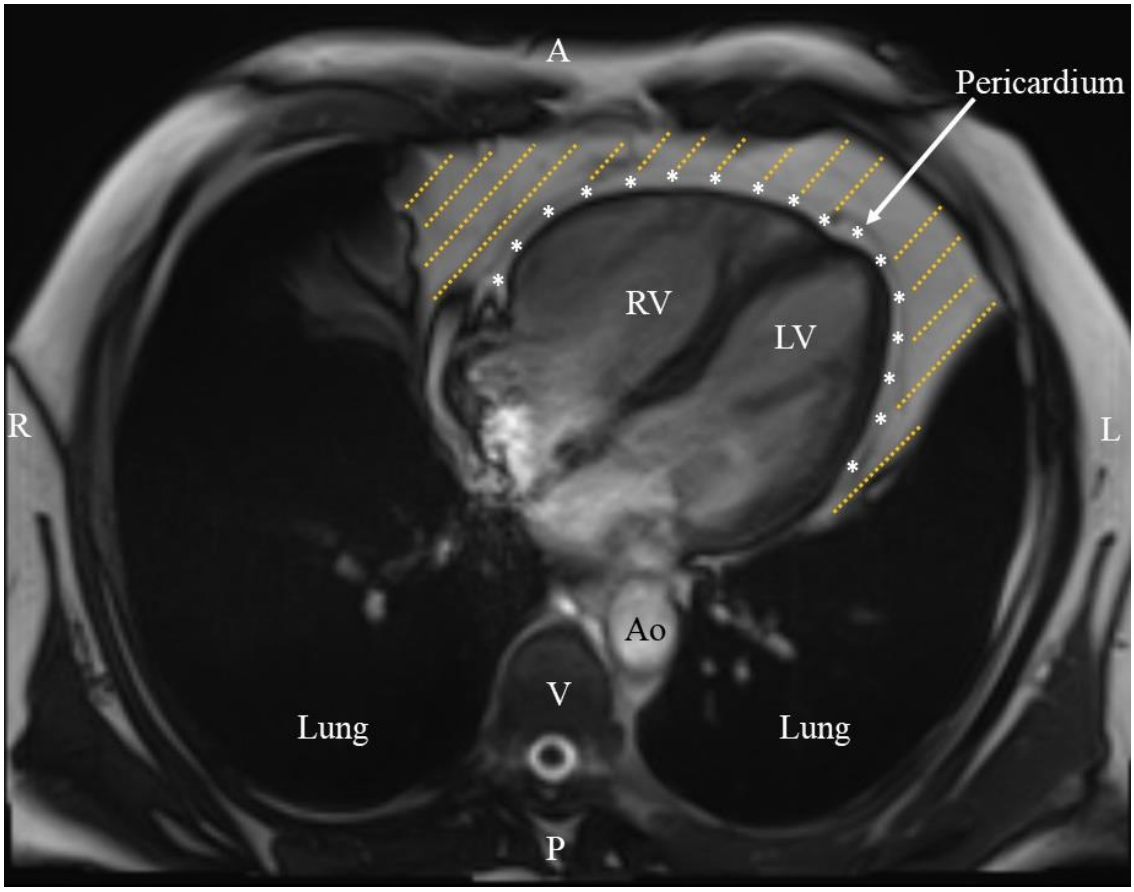

Figure 1: The pericardial fat depots

Magnetic Resonance (MR) image of the thorax in the axial orientation. The heart is shown in the long axis. Epicardial fat (white asterisks) and paracardial fat (orange dotted lines) are separated by the pericardium (white arrow). The sum of epi- and paracardial fat is referred to as pericardial fat. Abbreviations: A, anterior; Ao, aorta descendens; L, left; LV, left ventricle; P, posterior; R, right; RV, right ventricle; V, vertebra.

Epicardial fat is the fat compartment in closest proximity to the myocardium, within the visceral pericardium (Bertaso et al. 2013). Epicardial fat and the myocardium are in close proximity without a separating fascia and both are supplied by the same coronary artery blood supply (Corradi et al. 2004). It should be pointed out that epicardial adipocytes are smaller in volume (Marchington et al. 1989) and size (Bambace et al. 2011) as compared to other fat depots. Epicardial fat contains cardiac ganglia (Arora et al. 2003) and can be infiltrated by inflammatory cells (Mazurek et al. 2003). It has been reported that epicardial fat thickness over the right ventricle is associated with right ventricle cavity size (Iacobellis 2009a) and that there is a muscle-fat ratio for each ventricle (Corradi et al. 2004).

The term **paracardial fat** is used to describe the fat compartment more distant from the heart and located outside the parietal pericardial layer (Bertaso et al. 2013). Other terms found in the literature that refer to paracardial fat are ‘mediastinal fat’ (Chen et al. 2015) or ‘intrathoracic fat’ (Thanassoulis et al. 2010a).

1.2.2. Physiology and pathophysiology

There are numerous physiological functions attributed to the **epicardial fat** depot. However, many functions are still not fully understood.

Epicardial fat has been shown to have an insulin-independent high uptake of fatty acids, as well as an insulin-stimulated high rate of lipogenesis (Marchington and Pond 1990). Based on these findings, it was hypothesized that the epicardial fat layer might serve in a buffer function to the myocardium by protecting it from high levels of free fatty acids while also supplying energy equivalents (Marchington and Pond 1990, Marchington et al. 1989). Notably, the epicardial fat depot does not decrease as fast as other body fat depots during exercise or weight loss surgery in type 2 diabetes (Jonker et al. 2013, van Schinkel et al. 2014). The expression of the mitochondrial uncoupling protein 1 is increased in epicardial fat, and it has thus been suggested that epicardial fat may also have a protective function against hypothermia (Sacks et al. 2009). Moreover, it is now known that epicardial fat has an endocrine function. Epicardial fat expresses and secretes over 100 cytokines (Swifka et al. 2008). In samples collected during elective coronary artery bypass grafting, interleukin-1β, interleukin-6, tumor-necrosis-factor and other cytokines have been detected (Mazurek et al. 2003). Paracrine, which is close communication of cells by chemical substances, as well as vasocrine signaling pathways have been discussed for the interaction with the myocardium, the vessels and epicardial fat with its different cellular components (Sacks and Fain 2007, Yudkin et al. 2005).

Although displaying many beneficial features, epicardial fat has also been reported to play a role in multiple pathological processes. Firstly, data suggest that epicardial fat is associated with coronary artery disease (CAD) (Iacobellis et al. 2011). In a large study

comprising 3,367 subjects without a history of CAD, epicardial fat was associated with progressing coronary artery calcification (Mahabadi et al. 2014). In a post-mortem study validated by autopsies, there was an association seen between epicardial fat volume and the extent of coronary stenosis (Sequeira et al. 2015). Notably, epicardial fat volume may also help to identify subjects at risk for coronary artery calcium burden (Yerramasu et al. 2012). Interestingly, epicardial fat also seems to play a role in myocardial relaxation (Vural et al. 2014, Dabbah et al. 2014) and has been reported to be increased in patients who suffered from myocardial infarction (Homsi et al. 2018).

Moreover, epicardial fat has an impact on the electrophysiology of the heart and may play a role in atrial fibrillation. *Iacobellis et al* noted, that epicardial fat thickness, as assessed by echocardiography, was higher in subjects suffering from permanent, rather than paroxysmal atrial fibrillation (Iacobellis et al. 2014c). In the Framingham Heart Study, an independent association of epicardial fat with prevalent atrial fibrillation was detected (Thanassoulis et al. 2010b). It has to be pointed out that the Framingham Heart Study uses the word “pericardial fat” to describe the fat inside the pericardial sac which for this study is defined as “epicardial fat”. Additionally, epicardial fat seems to possess the ability to induce fibrotic changes of the myocardium (Venteclef et al. 2015).

Chronic obstructive pulmonary disease (COPD) can affect the heart as well. It has been shown that subjects suffering from COPD with advanced right ventricular systolic dysfunction had decreased epicardial fat thickness (Kaplan et al. 2015). Also, epicardial fat thickness is reported to be adversely associated with severity of COPD itself (Kiraz et al. 2016).

Epicardial fat seems to play a very important role in impaired glucose metabolism such as prediabetes and diabetes and these interactions will be discussed in a separate chapter of the introduction.

The physiological role of **paracardial fat** is not fully understood as of today. Only a few studies have investigated this particular fat compartment and found a correlation with visceral adipose tissue and metabolic risk factors (Thanassoulis et al. 2010a, Sicari

et al. 2011). A correlation between paracardial fat and coronary artery stenosis has been reported, but not as strongly as for epicardial fat (Sequeira et al. 2015).

Six months exercise decreased paracardial fat volume, as reported by *Jonker et al*, but not epicardial fat in type 2 diabetics (Jonker et al. 2013). Bariatric surgery clearly reduced the amount of paracardial fat to a greater extent than epicardial fat (van Schinkel et al. 2014, Wu et al. 2016).

1.2.3. Clinical relevance of epicardial fat

As described earlier, epicardial fat possesses a magnitude of beneficial but also several potentially adverse features. The full clinical relevance of epicardial fat is not fully understood as of today. Epicardial fat is discussed to be associated with CAD including non-calcified plaques (Alexopoulos et al. 2010), atrial fibrillation (Thanassoulis et al. 2010b), and it correlates with MR-derived signs for myocardial dysfunction in obese subjects with type 2 diabetes (Evin et al. 2016). It is increased in impaired glucose metabolism (Arpaci et al. 2015). Epicardial fat seems to influence established cardiometabolic risk factors such as hypertension (Teijeira-Fernandez et al. 2008), and glucose levels (Iacobellis et al. 2008a). In a combined positron emission tomography (PET) and computed tomography (CT) study, performed by *Janik et al*, epicardial fat measured on CT images was found to better predict ischemia than the established coronary artery calcium scoring test (Janik et al. 2010). Imaging of the epicardial fat compartment is easily performed by various imaging techniques as reviewed by *Davidovich et al* (Davidovich et al. 2013). Despite its relevance, assessment of epicardial fat volume or thickness is so far not routinely practiced in the general work-up of subjects at risk for cardiometabolic diseases.

Epicardial fat can also be the primary origin of thoracic pain in case of epicardial fat necrosis (Baig et al. 2012).

1.2.4. The role of epicardial fat in obesity and impaired glucose metabolism

Impaired glucose metabolism is, along with central obesity, disturbances in lipid metabolism and hypertension, a feature of the metabolic syndrome. This symptom complex is attributed to the Western lifestyle as shown by *Rodriguez-Monforte et al* (Rodriguez-Monforte et al. 2017). It has become clear that it is rather VAT that is associated with the development of impaired glucose metabolism (Neeland et al. 2012). VAT correlates well with epicardial fat as described by *Iacobellis et al* in 2003. They stated that epicardial fat assessed by echocardiography can be suggested as a predictor for VAT (Iacobellis et al. 2003). This correlation may be particularly true for obese subjects with diabetes (Jain et al. 2015, Levelt et al. 2016). Moreover, epicardial fat thickness has also been suggested as an indicator for obesity (Song et al. 2015). *Vasques et al* used ultrasound to measure the sagittal abdominal diameter and found that epicardial adipose tissue could be estimated by employing this parameter (Vasques et al. 2013). Moreover, epicardial fat thickness by ultrasound seems to predict hepatic steatosis in obesity (Iacobellis et al. 2014a).

Little is known about the interactions of epicardial fat and the early stages of impaired glucose metabolism. *Arpaci et al* found transthoracic echocardiographically assessed epicardial fat thickness to be elevated in prediabetes as compared to subjects with normal glucose tolerance (Arpaci et al. 2015). Also, epicardial fat has been discussed as a marker for cardiovascular disease risk in subjects with prediabetes (Altin et al. 2016). Insulin resistance has been shown to be an independent predictor of epicardial fat thickness (Altin et al. 2017). This finding has also been described in coronary artery disease (Baldasseroni et al. 2013). Interestingly, *Iacobellis and Leonetti* were able to show that epicardial fat assessed by echocardiography was associated with insulin-resistance due to obesity (Iacobellis and Leonetti 2005). Components of the metabolic syndrome are also associated with epicardial fat (Wang et al. 2009).

Epicardial fat has been shown to be elevated in subjects with type 2 diabetes (Song et al. 2015, Cetin et al. 2013, Wang et al. 2009). In a cross-sectional study conducted in

Korea, *Chun et al* found that an increased epicardial fat thickness has an impact on the diabetes prevalence in males (Chun et al. 2015). Moreover, in subjects with diabetes, epicardial fat displayed a more proinflammatory profile than in healthy controls and adipocytes were found to be larger than in the control group (Bambace et al. 2014). Additionally, miRNA expressed by epicardial fat, seems to play a role in coronary artery disease in subjects with type 2 diabetes (Liu et al. 2016).

Briefly, it should be pointed out that higher amounts of epicardial fat were also reported in type 1 diabetics as compared to healthy controls (Iacobellis et al. 2014b).

1.2.5. Imaging of the pericardial fat depots

The pericardial fat depots can be assessed by different imaging techniques including ultrasound, computed tomography (CT) and magnetic resonance imaging (MRI), although there is currently no single gold-standard (Davidovich et al. 2013). Non-radiological analysis like autopsy studies have also been performed and contributed to a better understanding of the fat depots (Sequeira et al. 2015).

Echocardiography is an easily accessible, cost-effective tool for the assessment of pericardial fat depots. Normally, epicardial fat can be assessed in parasternal long-axis and short-axis views; clinical applications have further been reviewed by *Iacobellis and Willens* (Iacobellis and Willens 2009b). Potentially hazardous epicardial fat thickness threshold values have also been evaluated by *Iacobellis et al* (Iacobellis et al. 2008b). Agreements between echocardiographically assessed epicardial fat and epicardial fat from MRI are good (Iacobellis et al. 2003). However, echocardiography is limited in adipose patients and is a very subjective imaging technique that highly depends on the operator.

Computed tomography (CT) has been widely used to assess pericardial fat depots. This modality has been shown to be feasible (Sarin et al. 2008) and highly reproducible in the volumetric assessment of epicardial fat (Gorter et al. 2008). The assessment of the different pericardial fat compartments is dependent on the identifiability of the thin pericardium. The administration of contrast agent is, however, not necessary for this distinction (Cheng et al. 2010). Today, computer-assisted assessment promises reliable and fast measurement of cardiac fat depots (Ding et al. 2015). CT has been applied for the assessment of pericardial fat depots in large studies such as the Framingham Heart Study (Rosito et al. 2008, Thanassoulis et al. 2010a, Thanassoulis et al. 2010b) or the Heinz Nixdorf Recall study (Mahabadi et al. 2014). However, the employment of CT is always linked to radiation exposure of the mostly healthy study subjects.

Cardiac magnetic resonance (CMR) imaging has also been employed for the assessment of pericardial fat depots. MRI provides a high soft tissue contrast and therefore plays a very important role in fat imaging. It has for example been employed in research concerning whole-body adipose tissue profiles (Machann et al. 2005). MRI – in comparison to CT – does not require ionizing radiation. MRI-based exams as well as CT tend to be more operator-independent than echocardiography (Wang et al. 2003). Volumetric (Flüchter et al. 2007) as well as thickness measurements (Iacobellis et al. 2003) have been conducted so far; however, study results indicate that the volumetric approach has a better interobserver variability (Flüchter et al. 2007). Pericardial fat volume assessment by MRI has been validated against postmortem studies in merino sheep, thereby establishing MRI is an important diagnostic tool (Nelson et al. 2009). Images can be acquired in four-chamber view orientation (Jonker et al. 2013) or in the short axis (Chen et al. 2015). It has been shown that MRI-based cardiac fat mass as assessed in a volumetric approach on short axis views correlates very well with planimetric assessment of cardiac fat derived from long axis images (Sironi et al. 2012). Studies on scanners with 3 Tesla magnets have also been conducted in the last years (Gaborit et al. 2012).

Analysis of the fatty acid composition of different fat depots including epicardial fat has been conducted by proton nuclear **MR spectroscopy** (Burgeiro et al. 2016).

Epicardial fat has also been assessed in **PET/CT** and its relationship to myocardial ischemia was analyzed (Janik et al. 2010).

1.3. Aim and scientific hypothesis

Subjects with impaired glucose metabolism and diabetes are at considerable risk for developing cardiovascular disease (Kannel and Mcgee 1979). However, the underlying detailed pathophysiology is highly complex. It is also known that certain body fat depots such as VAT play a role in impaired glucose metabolism and metabolic alterations (Lemieux et al. 2011, Hayashi et al. 2003, Fox et al. 2007). The ectopic fat depot epicardial fat has recently emerged as a potential correlate for cardiovascular risk (Rosito et al. 2008). Earlier cohort studies often employed radiation-based CT (Mahabadi et al. 2009, Mahabadi et al. 2014). Due to its high soft-tissue contrast and non-ionizing image generation, MRI is suitable for large cohort studies. Also, assessment of epicardial fat has been described as feasible in MRI (Flüchter et al. 2007). It is clear that the trend in imaging cohort studies including thousands of healthy subjects is shifting towards MRI (Gatidis et al. 2017) and that there will be an increasing need to analyze body structures on these images. Future applications for assessment of the pericardial fat compartments could include not only epidemiological research but also approaches in individualized medicine.

The aim of the underlying study was to manually assess the pericardial fat depots on MR images in the cine steady state free precession (SSFP) sequence, long axis (four chamber view), in a clinically cardiovascular healthy cohort. We aimed at comparing measurements from the systolic and diastolic assessment. Epicardial and paracardial fat depots were then analyzed in the light of impaired glucose metabolism as well as in relation to other MRI-derived body fat depot measurements and traditional cardiovascular risk factors. We also aimed at analyzing the association between epi-and paracardial fat and imaging-based LV parameters for subclinical LV dysfunction. Parts of this study aim have been previously published (Rado et al. 2019).

Our hypothesis was that assessing pericardial fat depots on MR images in the cine SSFP sequence is feasible for assessing the pericardial fat depots in both the systolic and diastolic heart cycle. We hypothesized that there are differences in epi- and paracardial fat between subjects with normal glucose tolerance and subjects with prediabetes and diabetes that allow for a more detailed characterization of their role in impaired glucose metabolism. Also, we hypothesized that there are independent associations between MR-based markers for early LV impairment and epicardial fat.

2. Material and Methods

2.1. Study population

The KORA study – short for "Kooperative Gesundheitsforschung in der Region Augsburg" (Cooperative Health Research in the Region Augsburg) - is a follow-up of the MONICA (Monitoring Trends and Determinants in Cardiovascular Disease) Augsburg surveys that were conducted by the WHO in the 1980s and 1990s in the Augsburg region (Löwel et al. 2005). The KORA study was initiated in 1996 as a follow-up epidemiological study with a focus on cardiovascular risk and metabolic diseases. The detailed study set up has been described by *Holle et al* (Holle et al. 2005). The history and structure of the KORA study is depicted in Figure 2.

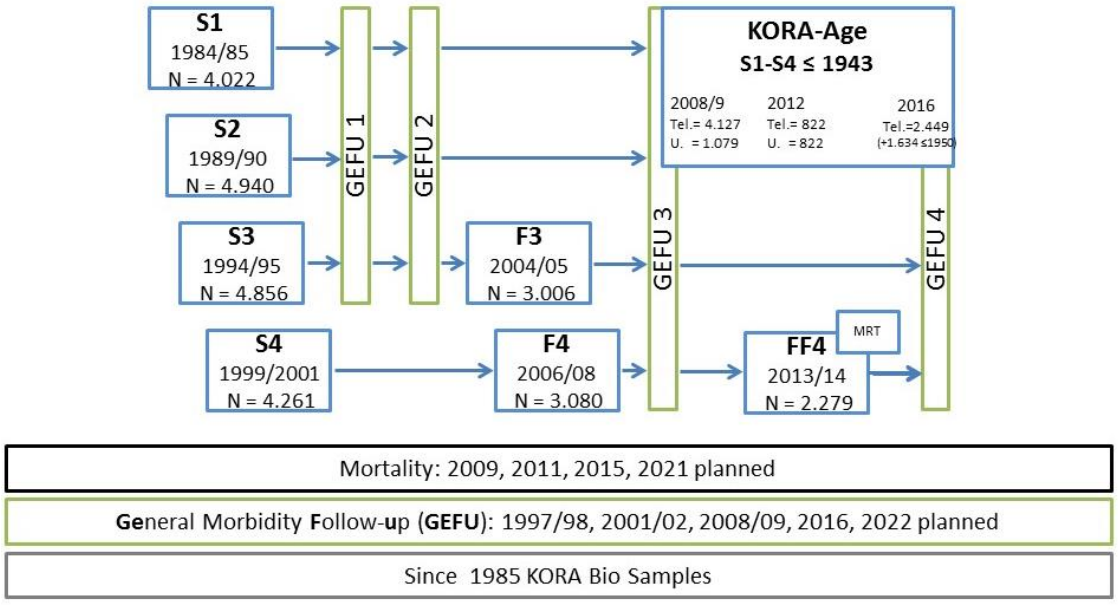

Figure 2: Overview of the KORA study

This figure shows an overview of the KORA study including the MRI study (depicted as 'MRT') which is nested within the KORA FF4 cohort, a follow up of the original S4 cohort. Abbreviations: GEFU, General (Morbidity) Follow Up; MRT, Magnetic Resonance Tomography; Tel, Telephone interview; U, Untersuchung (examination). This image is a courtesy of KORA Studien Koordination, Institut für Epidemiologie II, Helmholtz Zentrum München, Germany.

The KORA MRI sub-study is nested within the KORA FF4 cohort and subjects were recruited between 2013/2014. Female and male subjects aged 25-74 years were included. The study details regarding inclusion and exclusion criteria for the MRI sub-study have been outlined in a previous publication (Bamberg et al. 2017). In brief, subjects were eligible for participation if they had an established glucose tolerance status (either previously diagnosed diabetes or results of an OGTT). Exclusion criteria included age greater 72 years, history of clinically significant cardiovascular disease, inability to undergo MRI exams (e.g. implants, claustrophobia), pregnancy or lactation, or missing OGTT results. Moreover, subjects with contraindications for undergoing contrast-enhanced MRI exams were also excluded from the study (e.g. renal impairment with serum creatinine ≥1.3mg/dl, allergies to gadolinium-based contrast). Before participating in the MRI examination, informed written consent was obtained from each study subject. Ethical approval was also collected from the institutional review board of the Medical Faculty of the Ludwig Maximilians University Munich, Germany (Bamberg et al. 2017, Rado et al. 2019) under the project number 498-12. This ethical approval was reviewed and confirmed by the institutional review board of the Medical Faculty of the Eberhard Karls University Tübingen, Germany under the project number 576/2016BO2.

Subjects without an established diagnosis of diabetes underwent an OGTT. Glucose tolerance status was determined according to WHO recommendations: diabetes was defined as fasting plasma glucose ≥7.0 mmol/l (126 mg/dl) or 2-hour plasma glucose ≥11.1 mmol/l (200 mg/dl). IGT was defined as fasting plasma glucose <7.0 mmol/l (126 mg/dl) and 2-hour plasma glucose ≥7.8 and <11.1mmol/l (140-200mg/dl). IFG was defined as fasting plasma glucose 6.1 to 6.9 mmol/l (110 to 125 mg/dl) and 2-hour plasma glucose <7.8 mmol/l (140 mg/dl) (World Health Organization and International Diabetes Federation 2006).

Further health-related information, including physical exams, blood samples and interviews, was performed at dedicated study centers in an established and standardized fashion between 2013 and 2014 (Bamberg et al. 2017). Collection of relevant covariables will be described later.

2.2. MR imaging parameters

The complete study protocol for the KORA MRI study including the imaging parameters for the different sequences has been described in the study overview (Bamberg et al. 2017). In brief, the KORA MRI study focuses on cardiovascular imaging as well as assessment of different body fat compartments. Subjects included in this study underwent whole-body MRI with a pre-set protocol including multiple imaging sequences. Image acquisition was performed using a 3 Tesla Magnetom Skyra MRI (Siemens Healthineers, Erlangen, Germany) (Bamberg et al. 2017).

For the single-slice analysis of the pericardial fat depots, a cine steady-state free precession (SSFP) sequence in the long axis of the heart (four chamber view) was employed with the imaging parameters as follows: time-to-repetition (TR) 29.97 ms, time-to-echo (TE) 1.46 ms, field-of-view (FOV) 297 x 360 mm, slice thickness 8 mm, matrix 240 x 160, spatial resolution 1.5 x 1.5 mm^2, flip angle 63° (Bamberg et al. 2017).

The volumetric analysis of pericardial fat**,** VAT and SAT was conducted in a dual-echo volume interpolated breath hold examination (VIBE) Dixon sequence with the following imaging parameters: TR 4.06 ms, TE 1.26, 2.49 ms, FOV 488 x 716 mm, slice thickness 1.7 mm, matrix 256 x 256, spatial resolution 1.7 x 1.7 mm^2, flip angle 9° (Bamberg et al. 2017).

Further cardiac imaging included a short-axis cine SSFP sequence with the following imaging parameters: TR 29.97 ms, TE 1.46 ms (10sl), FOV 297 x 360 mm, slice thickness 8 mm, matrix 240 x 160, spatial resolution 1.5 x 1.5 mm^2, flip angle 62°, as well as a Fast Low Angle Shot (FLASH) sequence with the following parameters: TR 700-1000 ms, TE 1.55 ms, TI (inversion time) 280-345 ms, FOV 300 x 360, slice thickness 8 mm, matrix 256 x 140, spatial resolution 1.4 x 1.4 mm^2, flip angle 20-55° (Bamberg et al. 2017).

The proton-density fat fraction of the liver ($PDFF_{hepatic}$) was assessed in a multi-echo VIBE Dixon sequence during a 15 second breath hold with imaging parameters as follows: TR 8.90 ms, TE 1.23, 2.46, 3.69, 4.92, 6.15, 7.38 ms, FOV 393 x 450 mm, slice thickness 4 mm, matrix 256 x 179, spatial resolution 1.8 x 1.8 mm^2, flip angle 4 ° (Bamberg et al. 2017).

2.3. MR image analysis

Pericardial fat depots (single-slice approach): Image analysis was conducted employing a software (OsiriX Lite, Pixmeo SARL, Bernex, Switzerland). The MR images were manually imported into the software. For measurements of the fat areas, the tool called ‘polygonal region of interest (ROI)’ was employed. The pericardium was individually identified. Epicardial fat was segmented manually between the myocardium and the pericardium while small structures embedded in the adipose tissue (e.g. the coronary arteries) were not segmented separately. The pericardial fat compartment was segmented following the anatomical borders of the myocardium, lungs, aorta and ventral thoracic wall. Small structures embedded in the adipose tissue were also not segmented separately. Epi- and pericardial fat areas were assessed in the maximal systolic and diastolic heart cycle which were individually identified (Rado et al. 2019) (Figure 3).

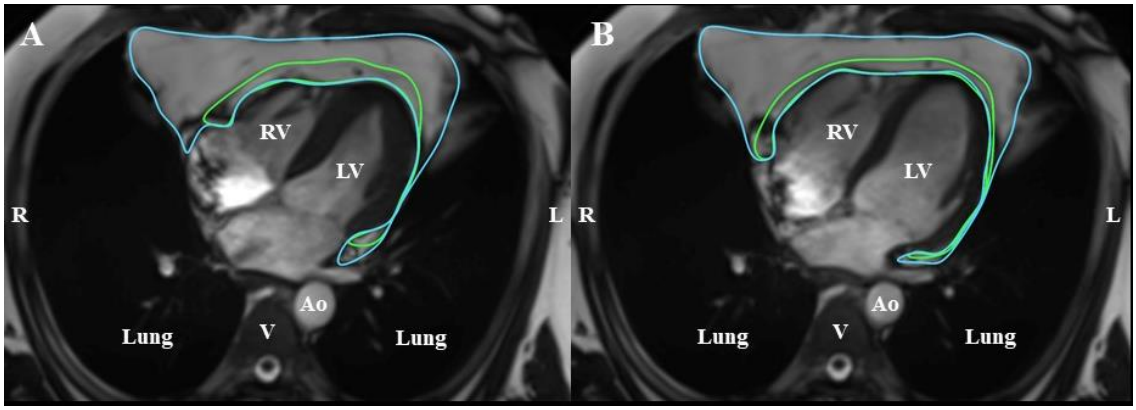

Figure 3: Assessment of the epicardial and pericardial fat compartments

Manual assessment of the pericardial (blue line) and the epicardial (green line) fat depots in the systolic (A) and the diastolic (B) heart cycle on images derived from the cine SSFP sequence in the long axis (four chamber view). The amount of paracardial fat was calculated by subtraction following segmentation (Rado et al. 2019). Abbreviations: Ao, aorta descendens; L, left; LV, left ventricle; R, right; RV, right ventricle; V, vertebra.

The areas of the pericardial and epicardial fat depots were recorded in centimeters squared [cm^2] and the results were documented in an Excel sheet (Microsoft, Redmond, Washington, USA). The amount of paracardial fat was determined by subtraction following the formula: paracardial fat = pericardial – epicardial fat (Rado et al. 2019). Additionally, image quality was evaluated on a five-point Likert scale with 1 = 'very good' to 5 = 'not assessable'. A final consensus reading was performed to rule out gross reading mistakes. Additionally, intra- and interreader reproducibility were assessed in a cohort subset of N=38. Throughout the reading process, readers were blinded with regards to subject identity and health status (Rado et al. 2019).

Pericardial Fat (volumetric approach): From the acquired dual-echo Dixon images, automatically calculated fat-selective tomograms were employed for further analysis. MR images were visualized on an offline workstation (SyngoVia, Siemens Healthineers, Forchheim, Germany) and axial tomograms were reconstructed automatically with a slice thickness of 2.5 mm, seamless. Pericardial fat was segmented from the diaphragm to the pulmonary bifurcation by manually selecting the slices. Between 28 and 36 slices were included for this analysis, based on the individuals'

anatomical heart sizes. The reconstructed tomograms were exported to a workstation and were reworked with an inhouse algorithm (Figure 4). Segmentations were corrected manually if necessary. Results are given in milliliters (ml) (J. Machann, personal communication).

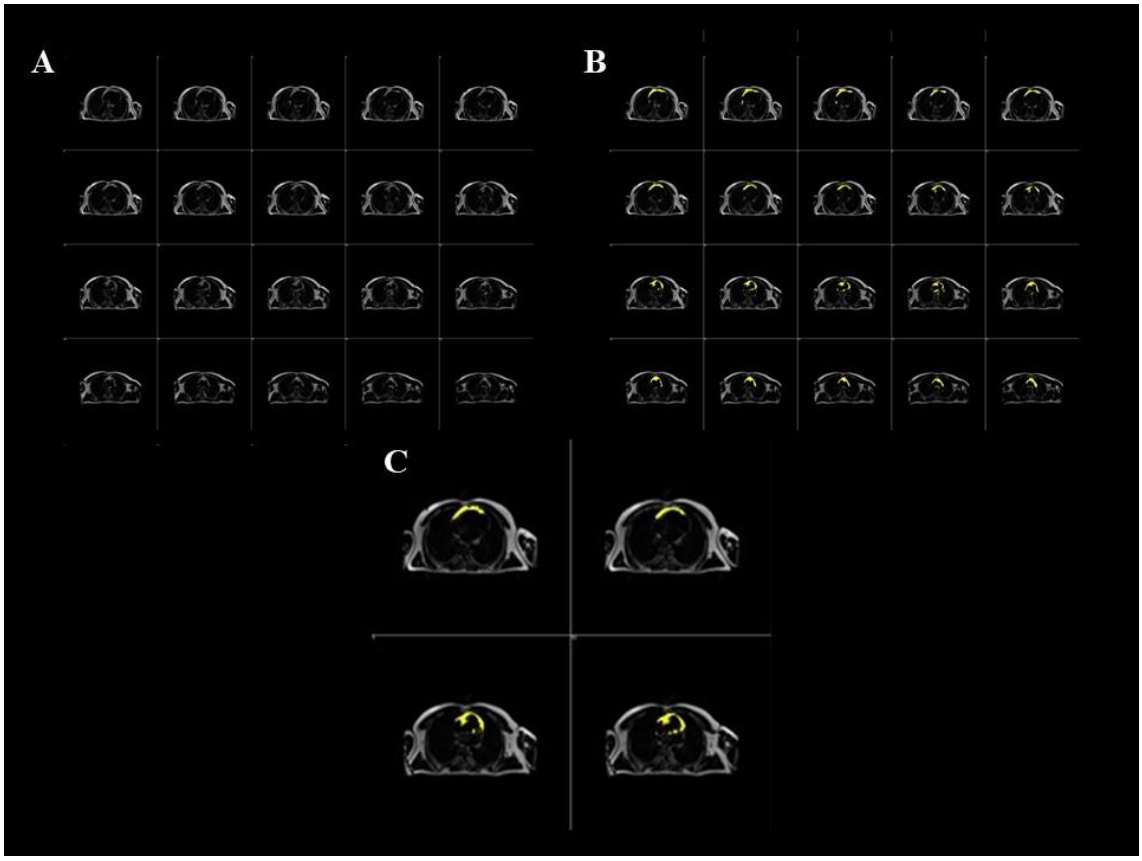

Figure 4: Principle of semiautomatic volumetric segmentation of pericardial fat

This figure shows the fat-selective axial tomograms of one study subject as reconstructed from the dual-echo Dixon sequence before (A) and after (B) semiautomatic segmentation of pericardial fat (yellow). Figure 4C is a magnification view of the segmented pericardial fat on four different levels. This image material is a courtesy of PD Dr Jürgen Machann, Section on Experimental Radiology, Department of Diagnostic and Interventional Radiology, University Hospital Tübingen, Tübingen, Germany.

VAT/SAT: VAT and SAT were analyzed on the fat-selective tomograms of the dual-echo VIBE Dixon sequence. A multiplanar reconstruction of the coronal data set into axial tomograms was performed from the femoral heads to the shoulders. The volumetric assessment of VAT was conducted between the femoral heads and cardiac

apex. The assessment of SAT was conducted between the femoral heads and diaphragm (Storz et al. 2018). An inhouse algorithm based on fuzzy-clustering (Würslin et al. 2010) was employed to semi-automatically assess VAT and SAT (Figure 5). The segmentation was corrected manually if necessary (Storz et al. 2018). Results are displayed in liters.

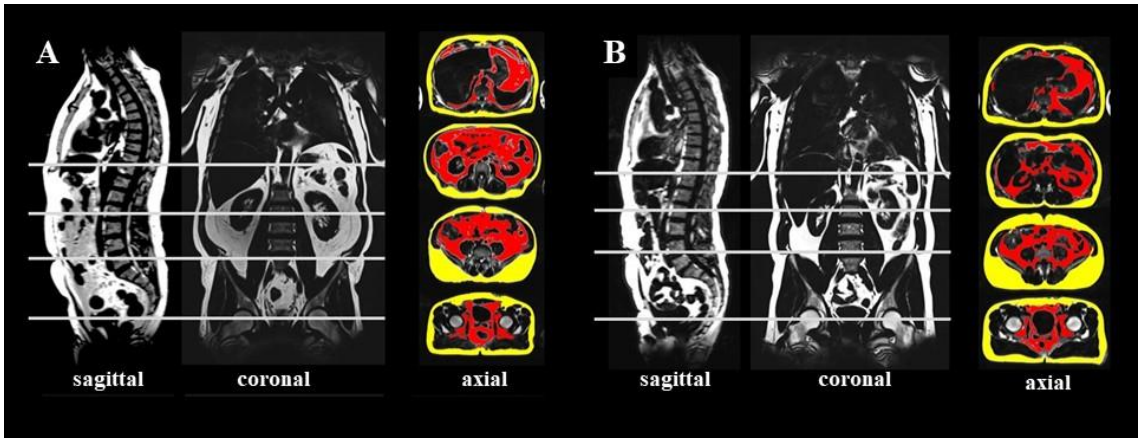

Figure 5: Principle of visceral (VAT) and subcutaneous (SAT) adipose tissue assessment

Fat-selective axial tomograms were reconstructed from coronal MR images (levels indicated by white lines on the sagittal and coronal images). VAT (red) and SAT (yellow) were automatically segmented. Figure A shows a study subject with a larger, and figure B with a smaller amount of VAT. This image material is a courtesy of PD Dr Jürgen Machann, Section on Experimental Radiology, Department of Diagnostic and Interventional Radiology, University Hospital Tübingen, Tübingen, Germany.

$PDFF_{hepatic}$: As previously described, a ROI was placed into the hepatic tissue on the PDFF maps, thereby carefully avoiding big adjacent vessels (Hetterich et al. 2016). Results are displayed in per cent.

LV parameters included late gadolinium enhancement (LGE), LV ejection fraction (EF) as well as left ventricular concentricity index (LVCI) which includes myocardial mass and end-diastolic volume. Data for EF as well as LVCI were analyzed on SSFP images in the short axis (10sl) while LGE data were derived from FLASH short axis and a four-chamber view. Image analysis on the short-axis SSFP images was

performed in a semiautomated fashion as previously described by employing a software (cvi42, Circle Cardiovascular Imaging, Calgary, Canada) (Bamberg et al. 2017, Rado et al. 2019, Schlett et al. 2018). An EF of <55% was considered pathological (Ueda et al. 2015). The LVCI was derived from LV myocardial mass divided by LV end-diastolic volume (Pun et al. 2011). LVCI values greater than 1.3 g/ml were considered pathological (Gaasch and Zile 2011). LGE was analyzed subendocardially, midmyocardially and epicardially by two readers in a consensus (Bamberg et al. 2017). The presence of LGE was considered pathological (Wu et al. 2001). A composite endpoint of subclinical LV impairment was defined for further analysis and consisted of the presence of LGE and/or LVEF <55% and/or LVCI > 1.3 g/ml (Rado et al. 2019).

2.4. Covariables

Covariables were collected from standardized interviews, laboratory work and physical exams. The collection of the covariables has been previously described (Holle et al. 2005, Bamberg et al. 2017).

Body mass index (BMI) as anthropometric measure was calculated as weight by height squared [kg/m^2]. With regards to blood pressure, hypertension was diagnosed if systolic blood pressures were ≥ 140mmHg and diastolic blood pressures ≥ 90mmHg. Also, hypertension was defined as taking antihypertensives whilst being aware of the hypertension diagnosis. Medication considered antihypertensive included beta blockers, diuretics etc. according to recent recommendations. Antithrombotic medication comprised antiplatelet and anticoagulant medication. The intake of drugs such as statins and fibrates were considered as lipid-lowering medication. Alcohol consumption data were derived from interviews and are given in g/day. Smoking information was derived from standardized interviews and results were grouped in the categories never, ex- and current smoker (Bamberg et al. 2017). Laboratory parameters such as total cholesterol, high-density lipoprotein (HDL), low-density lipoprotein (LDL), or triglycerides were

derived from fasting blood samples and were assessed in a standardized fashion as described by *Seissler et al* (Seissler et al. 2012).

2.5. Statistical analysis

Intraclass correlation coefficients (ICC) were calculated for analysis of intrareader and interreader reproducibility. The correlation between the single-slice and volumetric approach to assess pericardial fat was calculated by Pearson's pairwise correlation coefficient.

Demographic, clinical and imaging-based data are shown for all included study subjects as well as for the subgroups 'normal glucose tolerance', 'prediabetes' and 'diabetes' and are shown as either median [25^{th};75^{th} percentile] for continuous data or number (percentage) for categorical data and differences amongst these subgroups were analyzed either by Kruskal-Wallis equality of population rank test for continuous data, and χ^2-test or Fisher's exact test for categorical data (Rado et al. 2019).

Pericardial fat depots in the systolic and diastolic measurements were described by giving the minimum, maximum and quartiles including the median. Additionally, the median [25^{th};75^{th} percentile] is given for the different pericardial fat depots in both systole and diastole for the female and male subgroups separately.

Correlations between cardiac fat data derived from systole and diastole were calculated by Pearson's pairwise correlation coefficient and are presented as scatterplots. Agreements between systolic and diastolic cardiac fat parameters were also evaluated by plotting relative differences in Bland-Altman-Plots.

Data for the pericardial fat depots for all study subjects included as well as the subgroups 'normal glucose tolerance', 'prediabetes' and 'diabetes' are presented as median [25^{th}; 75^{th} percentile] and p-values were analyzed by Kruskal-Wallis equality of population rank test. This analysis was conducted for the systolic and diastolic data. Additionally, boxplots depict the differences in systolic epicardial/paracardial fat between the subgroups (Rado et al. 2019).

Stepwise adjustment for potential confounders of the association between prediabetes and diabetes to epicardial/paracardial fat was performed by employing median regression analysis and data including β-coefficients, 95% confidence intervals and p-values are presented in a table format. Data were firstly adjusted for age and gender only, followed by adjustment for traditional cardiovascular risk factors (CVRF) which included hypertension, smoking, LDL and triglycerides. Additional adjustment included measures of body fat, namely BMI, SAT and VAT (Rado et al. 2019). A multivariate analysis of the relationship of epicardial/paracardial fat to cardiovascular risk factors was performed by employing median regression and data are presented in a table format including β-coefficients, 95% confidence intervals and p-values (Rado et al. 2019).

Boxplots depict the differences in epicardial/paracardial fat amounts between healthy subjects and subjects showing subclinical LV impairment (Rado et al. 2019). The relationship between epicardial/paracardial fat and LV impairment was analyzed in a median regression model and was stepwise adjusted for traditional cardiovascular risk factors including diabetes status and VAT (Rado et al. 2019).

Median regression models were employed since data for epicardial and paracardial fat were not evenly distributed (Rado et al. 2019).

P-values <0.05 were defined as statistically significant. Data were analyzed in Stata 14.1 (Stata Corporation, College Station, TX, U.S.A.) (Rado et al. 2019).

3. Results

3.1. General results

400 subjects were primarily enrolled in the KORA MRI study. Images with an image quality rated 1-4 were included. Subjects with an image quality rated “5” (not assessable) and subjects without available images were not included in the final analysis (28 subjects, 7%, respectively). Of these, 1% had incomplete acquisition of the cine SSFP sequence and 6% had insufficient image quality due to motion artifacts, FOV misalignment, incomplete data acquisition or inability to delineate the pericardium sufficiently. Thus, 372 subjects were included in the underlying analysis (93%) (Rado et al. 2019).

3.2. Quality management

We found higher intraclass correlation coefficients (ICC) for intrareader than for interreader reproducibility. Results are depicted in Table 1. In general, $ICC_{Intrareader}$ as well as $ICC_{Interreader}$ were higher for the systolic as compared to the diastolic measurements. Due to this finding, further statistical analyses were conducted with the systolic fat measurements (Rado et al. 2019) unless otherwise indicated.

Table 1: Intraclass correlation coefficients for intrareader and interreader reproducibility of epicardial and pericardial fat depots

This table depicts the intraclass correlation coefficients for intra- as well as interreader reproducibility for the epicardial and pericardial fat depots in both systole and diastole. These data have previously been published (Rado et al. 2019).

Intraclass correlation coefficients (ICC)	Systole	Diastole
$ICC_{Intrareader}$ (epicardial fat)	0.918	0.844
$ICC_{Intrareader}$ (pericardial fat)	0.985	0.979
$ICC_{Interreader}$ (epicardial fat)	0.884	0.765
$ICC_{Interreader}$ (pericardial fat)	0.927	0.888

There was a strong positive correlation seen between the systolic as well as diastolic single-slice pericardial fat measurement with the volumetric approach with a correlation coefficient of $r=0.74$, $p<0.001$.

3.3. Study population characteristics

Demographic data and clinical characteristics of the underlying study population are displayed in Table 2. Of 372 subjects included in the final analysis, 220 subjects had normal glucose tolerance, 100 were prediabetics and 52 were diabetics (Rado et al. 2019). All diabetic subjects included in this final analysis had type 2 diabetes (Rado et al. 2019). The median age in all subjects included was 57 years [49;64] and increased significantly from healthy controls to prediabetics and diabetics ($p<0.001$). Overall, 59.4% of the subjects included were male and the percentage of males increased from controls to the prediabetes and diabetes group (53.2%, 64% and 76.9%; $p=0.004$, respectively) (Rado et al. 2019).

With regards to cardiovascular risk factors, there was a significant increase from subjects with normal glucose tolerance to prediabetics and diabetics concerning BMI (26.6 kg/m^2 vs 29.4 kg/m^2 vs 30.4 kg/m^2; $p<0.001$), hypertension (22.3% vs 45% vs 71.2%; $p<0.001$), and triglycerides (95.5 mg/dl vs 136.5 mg/dl vs 177.82 mg/dl; $p<0.001$). Additionally, prediabetics and diabetics had lower HDL levels as compared to subjects with normal glucose tolerance ($p<0.001$). However, no significant differences were found for LDL and smoking ($p=0.09$ and $p=0.11$, respectively) (Rado et al. 2019).

With regards to body fat composition, subjects with prediabetes and diabetes had higher amounts of VAT, SAT and $PDFF_{hepatic}$ as compared to subjects with normal glucose tolerance (all $p<0.001$) (Rado et al. 2019).

In comparison to normoglycemic controls, intake of antihypertensive and lipid-lowering medication was higher in the prediabetic and diabetic group (both $p<0.001$) (Rado et al. 2019).

Table 2: Demographic and clinical characteristics of the included study subjects

Data are presented for the total study population as well as for the subgroups ‘normal glucose tolerance’, ‘prediabetes’ and ‘diabetes’. Absolute numbers (percentage) are given for categorical data and the median (25^{th}; 75^{th} percentile) is given for continuous data. Abbreviations: “*BMI, body mass index; HDL, high-density lipoprotein; LDL, low-density lipoprotein; PDFF, proton density fat fraction; SAT, subcutaneous adipose tissue; VAT, visceral adipose tissue”* (Rado et al. 2019). This table has previously been published in the British Journal of Radiology (Rado et al. 2019).

	All subjects	**Normal glucose tolerance**	**Prediabetes**	**Diabetes**	**p-value**
	N=372	**N=220**	**N=100**	**N=52**	
Age (years)	57 (49;64)	53 (47;62)	59 (51;66)	63.5 (58;69.5)	<0.001
Male gender (%)	221 (59.4%)	117 (53.2%)	64 (64%)	40 (76.9%)	0.004
BMI (kg/m^2)	27.99 (25.16; 31)	26.58 (24.25; 29.01)	29.43 (27.3; 33.82)	30.43 (27.12; 33.09)	<0.001
Hypertension (%)	131 (35.2%)	49 (22.3%)	45 (45%)	37 (71.2%)	<0.001
Antihypertensive medication (%)	97 (26.1%)	39 (17.7%)	32 (32%)	26 (50%)	<0.001

Antithrombotic medication (%)	8 (2.2%)	3 (1.4%)	4 (4%)	1 (1.9%)	0.32
HDL (mg/dl)	59.52 (48; 72)	62 (51; 77)	59.26 (49.72; 69.6)	48.16 (40.5; 61.2)	<0.001
LDL (mg/dl)	138 (116; 161)	136 (115.5; 162.5)	143.5 (123; 161.5)	130.5 (109.5; 150.5)	0.09
Triglycerides (mg/dl)	110.5 (77.28; 162.5)	95.5 (69.5; 129.69)	136.5 (98; 184.62)	177.82 (114.76; 273.09)	<0.001
Lipid lowering medication (%)	42 (11.3%)	15 (6.8%)	9 (9%)	18 (34.6%)	<0.001
SAT (l)	7.41 (5.53; 10.05)	6.75 (5.16; 8.88)	8.65 (6.35; 11.97)	8.65 (6.3; 11.27)	<0.001
VAT (l)	4.23 (2.69; 6.35)	3.14 (1.8; 4.72)	5.44 (3.97; 7.32)	6.88 (5.76; 8.45)	<0.001
$PDFF_{hepatic}$ (%)	4.77 (2.79; 12.21)	3.44 (2.2; 5.9)	11.6 (4.79; 17.93)	15.89 (6.86; 24.13)	<0.001

Smoking status					0.11
Never-smoker	136 (36.6%)	88 (40.0%)	32 (32.0%)	16 (30.8%)	
Ex-smoker	163 (43.8%)	84 (38.2%)	50 (50.0%)	29 (55.8%)	
Current-smoker	73 (19.6%)	48 (21.8%)	18 (18.0%)	7 (13.5%)	

MRI-derived data for LV-function parameters were available in 345 subjects; 208 of them had normal glucose tolerance, 93 were prediabetics and 44 were diabetics. Significant changes between the groups with different glucose tolerance status were seen for EF, myocardial mass, LV end-diastolic volume, and LVCI but not for LGE. Of the 345 subjects included in this sub-analysis, 93 had at least one of the components of the defined composite endpoint for subclinical LV impairment (27%, respectively) with 6 (1.7%) subjects showing more than one of these findings (Rado et al. 2019). There was an increase in the composite pathologic LV findings seen from healthy subjects to prediabetics and diabetics (16.8%, 35.5%, 56.8%, p<0.001; respectively) (Rado et al. 2019). Further details are shown in Table 3.

Table 3: Differences in early LV impairment as determined by MR image analysis between subjects with normal glucose tolerance, prediabetics and diabetics

Data are presented for all subjects included as well as for the subgroups 'normal glucose tolerance', 'prediabetes', and 'diabetes'. Numbers (percentage) are shown for categorical data and median (25^{th};75^{th} percentile) for continuous data. Abbreviations: *"EF, ejection fraction; LGE, late gadolinium enhancement; LV, left ventricular; LVCI, left ventricular concentricity index"* (Rado et al. 2019). This table has previously been published in the British Journal of Radiology (Rado et al. 2019).

	All subjects	**Normal glucose tolerance**	**Pre-diabetes**	**Diabetes**	**p-value**
	N=345	**N=208**	**N=93**	**N=44**	
LV EF (%)	70 (65;75)	70 (65;74)	72 (66;77)	69 (64;74)	0.03
LV EF <55%	14 (4.1%)	10 (4.8%)	0 (0%)	4 (9.1%)	0.01
LV myocardial mass (g)	141 (115;166)	127 (106;160)	151 (131;172)	148 (133;170)	<0.001

LV end-diastolic volume (ml/m^2)	66 (56;75)	69 (61;80)	60 (52;68)	55 (48;63)	<0.001
LVCI (g/ml)	1.06 (0.9;1.28)	0.99 (0.87;1.14)	1.22 (1.02;1.35)	1.30 (1.05;1.57)	<0.001
LVCI >1.3 g/ml	77 (22.3%)	26 (12.5%)	30 (32.3%)	21 (47.7%)	<0.001
LGE	8 (2.3%)	2 (1%)	4 (4.3%)	2 (4.6%)	0.06
LGE or LVCI >1.3 g/ml or LV EF <55%	93 (27%)	35 (16.8%)	33 (35.5%)	25 (56.8%)	<0.001

3.4. Pericardial fat depots in systolic and diastolic assessment

Within the 372 subjects assessed, systolic pericardial fat values ranged from 3.3 cm^2 to 98.1 cm^2 with a median of 26.5 cm^2 and diastolic pericardial fat values ranged from 3.3 cm^2 to 83.0 cm^2 with a median of 23.6 cm^2. With regards to epicardial fat assessment, systolic epicardial fat values ranged from 0 cm^2 to 33.7 cm^2 with a median of 8.7 cm^2, and diastolic epicardial fat values ranged from 0 cm^2 to 32.1 cm^2 with a median of 7.7 cm^2. The calculated paracardial fat amount ranged from 1.3 cm^2 to 66.4 cm^2 with a median of 18.3 cm^2 in the systole, and from 1.6 cm^2 to 64.1 cm^2 with a median of 16.0 cm^2 in the diastole. Table 4 summarizes the above data. The median amounts of systolic epicardial and paracardial fat have been previously published (Rado et al. 2019).

Table 4: Pericardial fat depots in systolic and diastolic assessment

All 372 subjects were included. This table shows the minimum, 25th, 50th, 75th percentile as well as the maximum amount of epi-, para- and pericardial fat in the systolic and diastolic measurements. All numbers given are in centimeters squared (cm^2). Abbreviations: p, percentile

	minimum	**p25**	**p50**	**p75**	**maximum**
Pericardial fat (systole)	3.3	18.4	26.5	40.3	98.1
Pericardial fat (diastole)	3.3	15.9	23.6	35.8	83.0
Epicardial fat (systole)	0	5.6	8.7	11.2	33.7
Epicardial fat (diastole)	0	5.1	7.7	10.6	32.1
Paracardial fat (systole)	1.3	11.1	18.3	27.3	66.4
Paracardial fat (diastole)	1.6	9.7	16.0	25.4	64.1

Correlations between the systolic and diastolic data for pericardial, epicardial as well as paracardial fat were investigated and very strong correlations were found between the systolic and diastolic data for all fat depots with the highest correlation coefficient for pericardial fat (r=0.99 vs r=0.98 vs r=0.90, for pericardial, paracardial and epicardial fat, respectively; Figure 6).

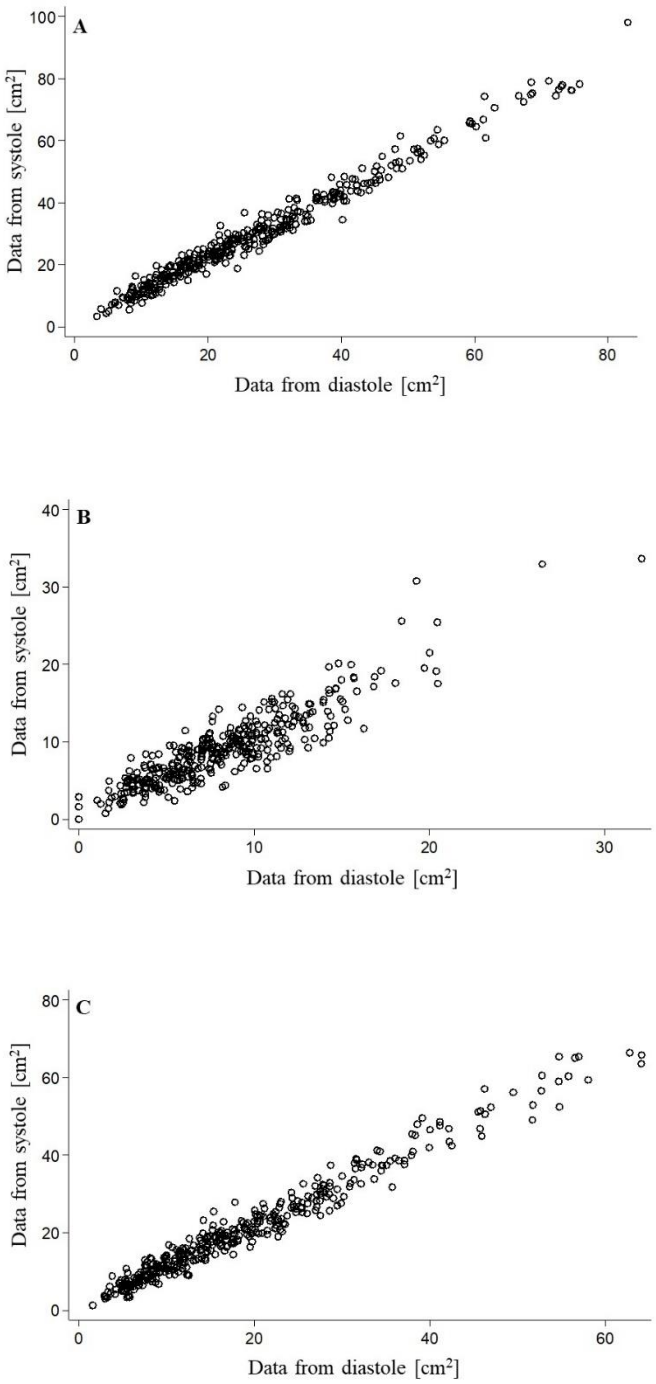

Figure 6: Correlations between the different pericardial fat depots in the systolic and diastolic heart cycle

This figure shows the correlations between the systolic (y-axis) and diastolic data (x-axis) for the pericardial (A), epicardial (B) and paracardial (C) fat depots.

Generally, data derived from systolic measurements were higher than from the diastolic measurements. In pericardial fat, the mean difference was 10.7%. In epicardial fat, the mean difference was 11.3%. For paracardial fat, the mean difference was 10.8%. Figure 7 depicts the agreements between systolic and diastolic measurements for the pericardial, epicardial and paracardial fat depots.

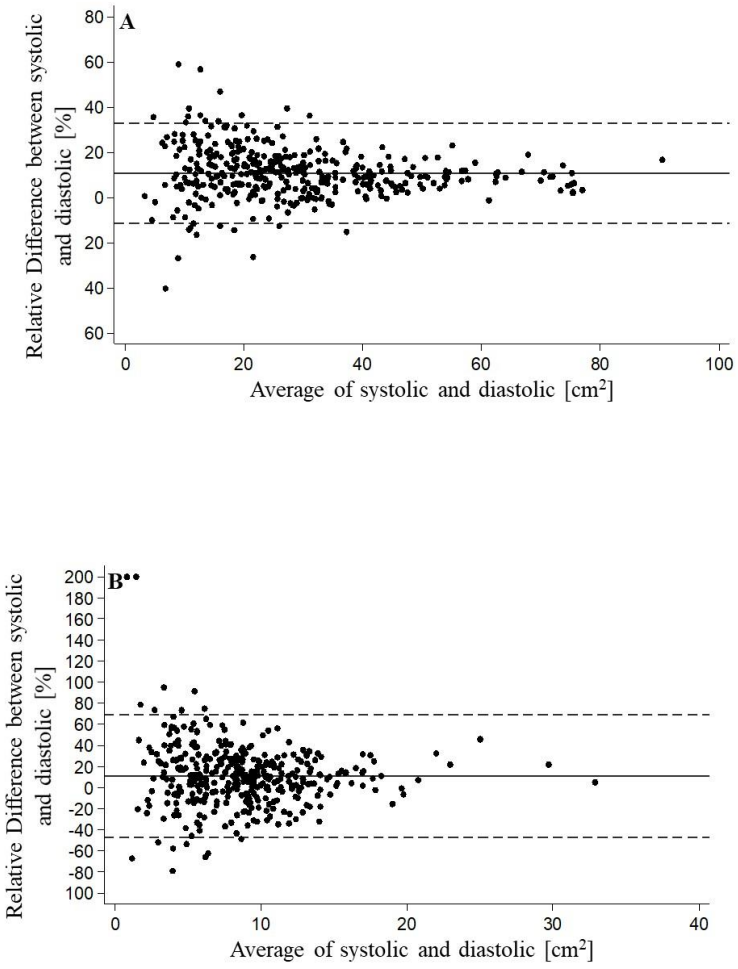

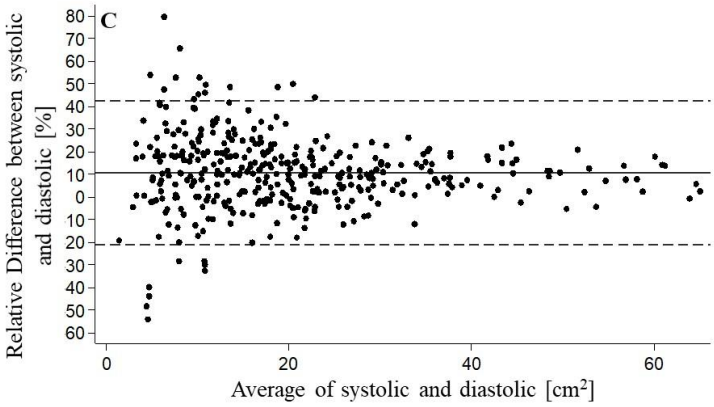

Figure 7: Agreements between systolic and diastolic measurements of the different pericardial fat depots

Agreements between the data sets derived from systolic and diastolic measurements for pericardial (A), epicardial (B) and paracardial (C) fat are presented as Bland-Altman plots. Relative differences are plotted in per cent on the y-axis and averages are given in centimeters squared on the x-axis.

In men, who accounted for 221 included subjects (59.4%, respectively), the median amount of epicardial fat in the systole was 9.2 cm^2 (6.7;12.2) and for women (151 subjects, 40.5%, respectively) 6.9 cm^2 (4.7;9.7). The median amount of epicardial fat in the diastole was 8.8 cm^2 (6.3;11.6) for men and 6.0 cm^2 (4.0;9.1) for women. The median amount of pericardial fat in the systole was 32.6 cm^2 (23.3;46.2) for men and 19.9 cm^2 (12.9;26.8) for women. The median amount of pericardial fat in the diastole was 30.8 cm^2 (21.5;42.4) for men and 17.1cm^2 (11.2;24.5) for women, respectively. For the calculated amount of paracardial fat, the median amount of paracardial fat in the systole was 23.1 cm^2 (16.0;33.9) for men and 11.7 cm^2 (7.8;17.5) for women, as well as 21.5 cm^2 (14.4;30.9) for men and 10.2 cm^2 (6.7;16.0) for women in the diastole. In general, all fat depots were larger in men as compared to women, irrespective of the systolic or diastolic measurements.

In the systole, there was a significant increase in median pericardial fat from healthy controls to prediabetics and diabetics (22.8 cm^2 vs 30.1 cm^2 vs 40.3 cm^2; $p<0.001$, respectively). Similar trends were seen for both the epicardial and paracardial fat depot separately (7.7 cm^2 vs 9.2 cm^2 vs 10.3 cm^2 and 14.3 cm^2 vs 20.3 cm^2 vs 27.4 cm^2; both $p<0.001$, respectively) (Rado et al. 2019); Table 5 and Figure 8).

Table 5: Differences in the pericardial fat depots as assessed in the systole between subjects with normal glucose tolerance, prediabetics and diabetics

Data are shown as median (25^{th}; 75^{th} percentile) and are displayed in centimeters squared [cm^2]. Data from the table have been partially published (Rado et al. 2019).

	All subjects	**Normal glucose tolerance**	**Prediabetes**	**Diabetes**	**p-value**
	N=372	**N=220**	**N=100**	**N=52**	
Pericardial fat [cm^2]	26.5 (18.4;40.3)	22.8 (14.6;32.1)	30.1 (22.8;43.5)	40.3 (29;53.6)	<0.001
Epicardial fat [cm^2]	8.7 (5.6;11.2)	7.7 (5;10.3)	9.2 (6.9;11.8)	10.3 (7.6;14.4)	<0.001
Paracardial fat [cm^2]	18.3 (11.1;27.3)	14.3 (9;22.5)	20.3 (15.5;30.1)	27.4 (20.7;37.8)	<0.001

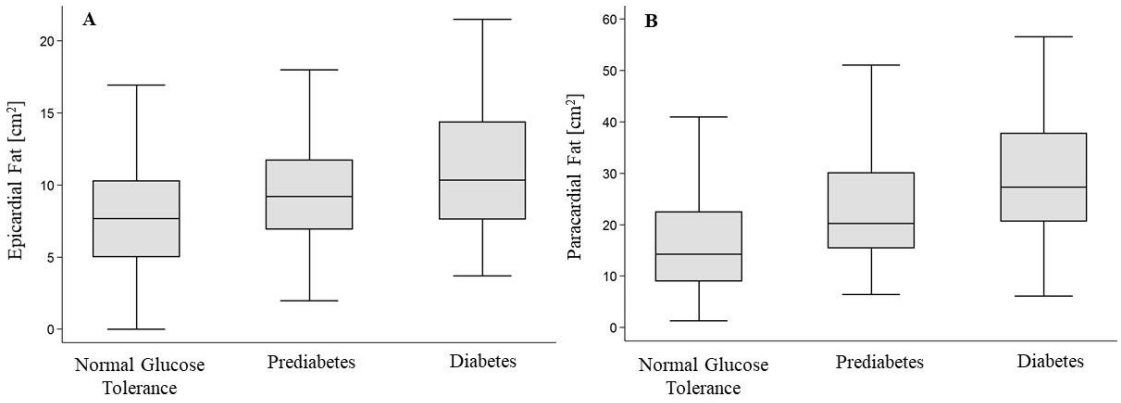

Figure 8: Differences between epicardial and paracardial fat in subjects with normal glucose tolerance, prediabetics and diabetics

Boxplots depicting the stepwise increase in both systolic epicardial (A) and systolic paracardial (B) fat from healthy subjects to prediabetics and diabetics. All p were <0.001. The fat amounts are presented in centimeter squared [cm^2] on the y-axis. This figure has previously been published in the British Journal of Radiology (Rado et al. 2019).

Similar results were found for the diastolic assessment of the pericardial fat depots. Pericardial fat and both the epi- as well as paracardial fat depot increased from subjects with normal glucose tolerance to prediabetics and diabetics. Results are shown in Table 6.

Table 6: Differences in the pericardial fat depots as assessed in the diastole between subjects with normal glucose tolerance, prediabetics and diabetics

Data are shown as median (25^{th}; 75^{th} percentile) and are displayed in centimeters squared [cm^2].

	All subjects	**Normal glucose tolerance**	**Prediabetes**	**Diabetes**	**p-value**
	N=372	**N=220**	**N=100**	**N=52**	
Pericardial fat [cm^2]	23.6 (15.9;35.8)	20.0 (12.8;29.4)	26.2 (20.9;39.6)	38.0 (24.7;48.4)	<0.001
Epicardial fat [cm^2]	7.7 (5.1;10.6)	6.9 (4.4;9.7)	8.6 (5.9;11.1)	9.8 (7.5;13.3)	<0.001
Paracardial fat [cm^2]	16.0 (9.7;25.4)	12.4 (7.7;20.6)	18.7 (13.6;27.3)	26.2 (17.6;34.1)	<0.001

3.5. Adjustment for potential confounders

In an unadjusted setting, there was an association between epicardial fat and prediabetes as well as diabetes seen (both $p \leq 0.02$). After adjusting for age and gender, the association to prediabetes became non-significant (p=0.14) whereas epicardial fat was still associated with diabetes (p=0.02). The association attenuated for both the prediabetic and diabetic group after additionally adjusting for cardiovascular risk factors including hypertension, triglycerides, LDL and smoking (p=0.37 and 0.59, respectively) (Rado et al. 2019). Details are depicted in Table 7.

Table 7: **Stepwise adjustment for potential confounders of the association between epicardial fat with prediabetes and diabetes**

The systolic data for epicardial fat were employed for this analysis. Data are derived from median regression and are displayed as ß-coefficient (95% confidence interval) and p-value. P-values in bold are statistically significant. Abbreviations: *"BMI, body mass index; CI, confidence interval; CVRF, cardiovascular risk factor; LDL, low-density lipoprotein; SAT, subcutaneous adipose tissue; VAT, visceral adipose tissue"* (Rado et al. 2019). CVRF included hypertension, smoking, LDL and triglycerides. This table has previously been published in the British Journal of Radiology (Rado et al. 2019).

	Normal glucose tolerance	**Prediabetes**		**Diabetes**	
Epicardial fat		**β (95 CI)**	**p-value**	**β (95 CI)**	**p-value**
Unadjusted	-Ref.-	1.54 (0.23;2.84)	**0.02**	3.04 (1.39;4.68)	**<0.001**
Adjusted for					
Age, gender	-Ref.-	0.94 (-0.29;2.16)	0.14	1.98 (0.36;3.61)	**0.02**
Age, gender, CVRF	-Ref.-	0.55 (-0.66;1.76)	0.37	0.47 (-1.26;2.2)	0.59
Age, gender, CVRF, BMI	-Ref.-	0.3 (-0.87;1.47)	0.62	-0.08 (-1.71;1.56)	0.93
Age, gender, CVRF, SAT	-Ref.-	0.29 (-0.89;1.47)	0.63	0.35 (-1.3;2.01)	0.68
Age, gender, CVRF, VAT	-Ref.-	-0.41 (-1.55;0.73)	0.48	-0.92 (-2.53;0.7)	0.27

For **paracardial fat**, there was a significant association between paracardial fat and prediabetes as well as diabetes after adjustment for age and gender seen (p=0.01 and <0.001, respectively). The association became non-significant for the prediabetes group

after adjusting for age, gender and cardiovascular risk factors. A significant association was seen for the diabetes group after adjustment for age, gender, CVRF without (p=0.04) and with BMI (p=0.03), as well as after adjustment for age, gender, CVRF and SAT (p=0.048) (Rado et al. 2019). Details are depicted in Table 8.

Table 8: Stepwise adjustment for potential confounders of the association between paracardial fat with prediabetes and diabetes

The systolic data for paracardial fat were employed for this analysis. Data are derived from median regression and are displayed as ß-coefficient (95% confidence interval) and p-value. P-values in bold are statistically significant. Abbreviations: *"BMI, body mass index; CI, confidence interval; CVRF, cardiovascular risk factor; LDL, low-density lipoprotein; SAT, subcutaneous adipose tissue; VAT, visceral adipose tissue"* (Rado et al. 2019). This table has previously been published in the British Journal of Radiology (Rado et al. 2019).

	Normal glucose tolerance	**Prediabetes**		**Diabetes**	
Paracardial fat		**β (95 CI)**	**p-value**	**β (95 CI)**	**p-value**
Unadjusted	-Ref.-	5.15 (1.36;8.94)	**0.01**	13.08 (8.31;17.85)	**<0.001**
Adjusted for					
Age, gender	-Ref.-	4.45 (1.27;7.63)	**0.01**	8.77 (4.57;12.97)	**<0.001**
Age, gender, CVRF	-Ref.-	3.59 (-0.1;7.28)	0.06	5.43 (0.15;10.71)	**0.04**
Age, gender, CVRF, BMI	-Ref.-	1.77 (-1.34;4.88)	0.26	4.89 (0.54;9.24)	**0.03**
Age, gender, CVRF, SAT	-Ref.-	0.56 (-2.74;3.86)	0.74	4.68 (0.05;9.31)	**0.048**
Age, gender, CVRF, VAT	-Ref.-	-2.16 (-4.91;0.59)	0.12	-1.72 (-5.6;2.16)	0.39

In multivariate analysis, most traditional cardiovascular risk factors including age, hypertension or LDL were not significantly associated with either epicardial or paracardial fat. There was a strong association seen between VAT and epicardial as well as VAT and paracardial fat (β: 1.08 [0.76; 1.4], p<0.001; and β: 4.10 [3.32; 4.88], p<0.001, respectively). Furthermore, epicardial fat was associated with current smoking (β: 1.39 [0.07; 2.70], p=0.04). There was a negative association between paracardial fat and SAT seen (p=0.04) (Rado et al. 2019). Further details are given in Table 9.

Table 9: Multivariate analysis of the relationship between the epicardial and paracardial fat depots to cardiovascular risk factors including body fat depots

Systolic data for epicardial and paracardial fat were employed. Data are derived from median regression and are displayed as β-coefficient (95% confidence interval). Significant p-values are marked in bold font. Abbreviations: *"CI, confidence interval; HDL, high-density lipoprotein; LDL, low-density lipoprotein; PDFF, proton-density fat fraction; SAT, subcutaneous adipose tissue; VAT, visceral adipose tissue"* (Rado et al. 2019). This table has been previously published in the British Journal of Radiology (Rado et al. 2019).

	Epicardial fat		**Paracardial fat**	
	β (95%CI)	**p-value**	**β (95%CI)**	**p-value**
Age (years)	0.03 (-0.03; 0.09)	0.27	0.01 (-0.14; 0.15)	0.93
Male gender (%)	-0.72 (-2.14; 0.70)	0.32	0.87 (-2.57; 4.31)	0.62
Hypertension (%)	-0.48 (-1.55; 0.59)	0.38	0.71 (-1.88; 3.31)	0.59
LDL (mg/dl)	-0.01 (-0.03; 0.001)	0.08	0 (-0.04; 0.04)	1.00
HDL (mg/dl)	0.004 (-0.03; 0.04)	0.81	0.005 (-0.08; 0.09)	0.91
Triglyceride (mg/dl)	0.002 (-0.005; 0.008)	0.59	-0.002 (-0.02; 0.01)	0.8
Alcohol (g/day)	0.007 (-0.02; 0.03)	0.54	-0.03 (-0.08; 0.02)	0.29
Smoking				
Never-smoker	-Ref.-		-Ref.-	

Ex-smoker	0.8 (-0.23; 1.82)	0.13	-1.27 (-3.76; 1.23)	0.32
Current-smoker	1.39 (0.07; 2.70)	**0.04**	-1.45 (-4.64; 1.73)	0.37
VAT (l)	1.08 (0.76; 1.4)	**<0.001**	4.10 (3.32; 4.88)	**<0.001**
SAT (l)	-0.02 (-0.19; 0.16)	0.87	-0.46 (-0.89; -0.032)	**0.04**
$PDFF_{hepatic}$ (%)	-0.04 (-0.11; 0.03)	0.21	-0.17 (-0.33; 0.001)	0.05

3.6. Cardiac fat depots and early left-ventricular impairment

In general, subjects with early LV impairment as assessed on MR images, had significantly higher amounts of both epicardial and paracardial fat as compared to healthy subjects ($p<0.001$) (Rado et al. 2019) (Figure 9).

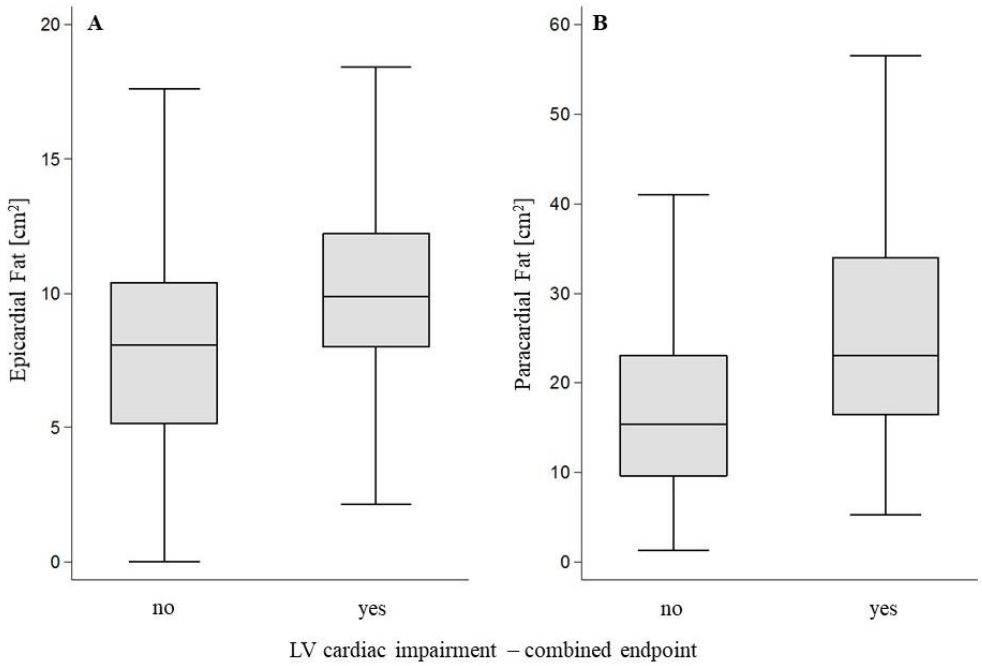

Figure 9: Differences between amounts of epicardial and paracardial fat in subjects with and without signs for left ventricular impairment

Epicardial (A) and paracardial (B) fat amounts in relation to signs of LV cardiac impairment (endpoint of LVEF<55%; presence of LGE; LVCI >1.3g/ml). Fat amounts are presented in centimeters squared [cm^2] on the y-axis. This figure has been previously published in the British Journal of Radiology (Rado et al. 2019).

In an unadjusted setting, both epicardial and paracardial fat were associated with the combined endpoint of LV impairment (p=0.004 and <0.001, respectively). The association between epicardial fat and LV impairment persisted after adjustment for cardiovascular risk factors including diabetes (β: 1.63 (0.5; 2.76), p= 0.005). The association even remained independent upon additional adjustment for VAT (β: 1.13 (0.22; 2.03), p=0.02) but became non-significant upon adjustment for BMI (p=0.09) (Rado et al. 2019).

For paracardial fat, loss of significance was seen after adjustment for diabetes status (p=0.13) (Rado et al. 2019). Further details on the stepwise adjustment are given in Table 10.

Table 10: Epicardial and paracardial fat and associations to signs for early LV impairment

Systolic data were employed for epicardial and paracardial fat and a stepwise adjustment for multiple variables was conducted. Data are presented as β-coefficient (95% confidence interval) and significant p-values are marked in bold font. Abbreviations: *"BMI, body mass index; CI, confidence interval; LDL, low-density lipoprotein; LV, left ventricular; VAT, visceral adipose tissue. LV impairment was defined as a combined endpoint of LGE, EF <55% or LVCI > 1.3 g ml^{-1}"* (Rado et al. 2019). This table has been previously published in the British Journal of Radiology (Rado et al. 2019).

	Epicardial fat		**Paracardial fat**	
LV impairment	**β (95 CI)**	**p-value**	**β (95 CI)**	**p-value**
Unadjusted	1.80 (0.57; 3.03)	**0.004**	6.9 (3.3; 10.49)	**<0.001**
Adjusted for				
Age, gender, smoking, hypertension, LDL	1.26 (0.18; 2.35)	**0.02**	4.92 (1.79; 8.05)	**0.002**

Age, gender, smoking, hypertension, LDL, diabetes	1.63 (0.5; 2.76)	**0.005**	2.63 (-0.75; 6.00)	0.13
Age, gender, smoking, hypertension, LDL, diabetes, BMI	0.95 (-0.15; 2.05)	0.09	1.63 (-1.63; 4.89)	0.33
Age, gender, smoking, hypertension, LDL, diabetes, VAT	1.13 (0.22; 2.03)	**0.02**	0.88 (-1.53; 3.30)	0.47

4. Discussion

In the present analysis, our aim was to investigate MRI-based, manually segmented, single-slice pericardial fat depots with a special emphasis on associations with impaired glucose metabolism and signs for subclinical left-ventricular impairment in a clinically cardiovascular healthy cohort from the general population (Rado et al. 2019). In summary, the manual assessment of epicardial and pericardial fat in the systolic and diastolic heart cycle was feasible when employing the cine SSFP sequence in the long axis (four chamber view). Higher inter-reader and intrareader reproducibility was found for systolic as compared to diastolic readings (Rado et al. 2019). A strong correlation was seen between the volumetric and the single-slice assessment of pericardial fat. Very strong correlations were found between systolic and diastolic measurements for all pericardial fat depots. In general, systolic measurements were higher than diastolic measurements. Men had higher amounts of all fat depots as compared to women and regardless of the systolic or diastolic measurements.

There were significant differences seen in the amounts of epicardial and paracardial fat between prediabetics, diabetics and controls. We found a significant increase in epicardial as well as paracardial fat from healthy subjects to prediabetics and diabetics (Rado et al. 2019). Upon stepwise adjustment for traditional cardiovascular risk factors including body fat depots, this association became non-significant for both epicardial and paracardial fat. Multivariate analysis revealed that VAT was the best predictor for epicardial as well as paracardial fat (Rado et al. 2019) whereas no significant association was found for other traditional cardiovascular risk factors.

Subjects with signs for early subclinical LV impairment as determined on MR images had significantly higher amounts of epicardial and paracardial fat (Rado et al. 2019). Epicardial fat was independently associated with MRI-derived signs for early LV impairment (endpoint: LVEF<55%; presence of LGE; LVCI >1.3g/ml) after adjusting for traditional cardiovascular risk factors including VAT, but a loss of significance was seen when adjusting for BMI instead of VAT. There was no independent association between paracardial fat and signs for LV impairment (Rado et al. 2019).

The manual assessment of the pericardial fat depots on MR images in the cine SSFP sequence was feasible (Rado et al. 2019). SSFP sequences are considered standard CMR sequences for analysis of especially the LV structure and function and are the preferred sequence for cine imaging (Kramer et al. 2013). Among others, SSFP imaging has been included in MR imaging protocols in emerging epidemiological studies including the German National Cohort (Bamberg et al. 2015) or the UK Biobank (Petersen et al. 2016). While labor-intensive and time-consuming, manual segmentation of the pericardial fat depots using this sequence has been found practicable in our approach; especially since the cine-sequence offers the possibility to assess the fat depots not only in one heart cycle but in the systole and the diastole. This finding is important as it allows for segmentation of the pericardial fat depots using standard images acquired during a whole-body MRI exam without employing an additional, specialized MRI sequence. Segmentation can only be conducted upon identification of the thin pericardium; however, identification was unsuccessful in only one data set of the 400 subjects included. The epicardial fat depot can then easily be detected as the fat located between the myocardium and the pericardium. In an attempt to avoid mistakes by overlapping ROIs, we opted to segment only the epicardial and the pericardial fat amounts and then deduct the amount of epicardial fat, thus obtaining the amount of paracardial fat. Similar approaches of segmenting only two of the fat depots and calculating the missing one by subtraction, have been described earlier (Thanassoulis et al. 2010a). Additionally, it needs to be pointed out that we did not segment small, non-fatty structures embedded in the pericardial fat depots separately. Thus, a minimal overestimation of the fat amounts cannot be ruled out in our study cohort. This attempt is in contrast to other approaches towards the fat assessment. In studies employing CT images for pericardial fat assessment, dedicated Hounsfield units were attributed to fat and the fat depots were then semi-automatically analyzed (Thanassoulis et al. 2010a). However, since we used our approach for all study subjects included in the final analysis, our data set can still be regarded as consistent within itself.

We found that the intraclass correlations were higher for the intrareader than for the interreader comparison. Similar results have been reported from the Framingham Heart Study (Rosito et al. 2008). This finding is expected and may stem from the routine an individual reader develops during the segmentation process. Intrareader as well as

interreader results were better for the pericardial as compared to the epicardial fat depots in both the systole and diastole. *Rosito et al* note the same finding of higher intraclass correlations for pericardial as compared to epicardial fat segmentation (Rosito et al. 2008), although they only segmented the fat depots in one heart cycle. This finding may be explained by the smaller size of the epicardial fat depot which may more easily result in segmentation errors. Interestingly, when comparing systolic and diastolic measurements, intrareader and interreader reproducibility were higher for the systolic measurements. This finding may be explained by better delineation and thus higher rates of agreement of the fat depots as the heart is contracted (Rado et al. 2019). In consideration of this finding, we decided to employ the systolic data in our statistical analysis (Rado et al. 2019), unless otherwise indicated.

A good correlation was found between manually assessed single-slice pericardial fat and automatically assessed volumetric pericardial fat. Similar results for a planimetric versus volumetric approach for the epicardial fat depot as derived from CT images have been reported by *Oyama et al* (Oyama et al. 2011). Additionally, *Sironi et al* found that cardiac fat mass correlated with the cardiac fat area from assessment in the four-chamber view in a cohort of N=20 healthy subjects (Sironi et al. 2012). Our finding can be seen as reassurance that the selected sequence, approach and segmentation technique are acceptable for pericardial fat assessment.

In our study, prediabetics and diabetics had a more unfavorable constellation concerning traditional cardiovascular risk factors such as the presence of hypertension or elevated triglycerides when compared to subjects with normal glucose tolerance (Rado et al. 2019). This finding may be due to impaired glucose metabolism being a part of the metabolic syndrome that is known as an array of disturbances in e.g. lipid metabolism and blood pressure (Grundy et al. 2004). There was an increase in the fat depots VAT, SAT, and $PDFF_{hepatic}$ from normoglycemic subjects to subjects with impaired glucose metabolism (Rado et al. 2019). It is well established that the accumulation of VAT is associated with an unfavorable cardiometabolic risk profile, even in healthy subjects (De Larochellière et al. 2014). In the Framingham Heart Study, *Fox et al* found VAT to be

associated with an adverse metabolic risk in 3001 subjects, independent of BMI or waist circumference (Fox et al. 2007). We found subjects with prediabetes and diabetes to be taking more cardioprotective medication such as antihypertensive or lipid-lowering medication than healthy controls (Rado et al. 2019). This finding needs to be taken into consideration when interpreting further results as these pharmaceuticals may influence the two investigated structures, namely body fat depots and cardiac function. Thus, our study results cannot be directly compared to drug-naïve individuals.

There was a significant increase seen in the composite endpoint of subclinical LV impairment (LVEF<55%; LVCI >1.3g/ml; presence of LGE) from subjects with normal glucose tolerance to prediabetics and diabetics in this clinically cardiovascular healthy cohort (Rado et al. 2019). As has been mentioned earlier, it is known that diabetes is one of the major contributors towards cardiovascular disease (Kannel and Mcgee 1979). Our results, in conjunction with other findings from the same cohort (Bamberg et al. 2017) show that cardiovascular alterations already occur in prediabetic stages, and that these subclinical changes can be visualized by MRI. Future applications for these findings might open new ventures for preventative medicine.

A significant increase in LV myocardial mass was noted in subjects with impaired glucose metabolism (Rado et al. 2019). This finding may be attributed to early structural changes of the myocardium in response to impaired glucose metabolism. An increase in LV mass in impaired glucose metabolism has previously been reported especially for women in the Framingham Heart Study by *Rutter et al* (Rutter et al. 2003). It is known that impaired glucose metabolism induces structural alterations such as increasing central artery stiffness (Schram et al. 2004).

Within the 372 data sets included in the final analysis, the epicardial fat depots assessed in both the systole and the diastole were smaller than the paracardial fat depots (Rado et al. 2019). An inverse relation has been reported from the Framingham Heart Study by *Mahabadi et al* (Mahabadi et al. 2009). *Sicari et al* measured epicardial and paracardial fat on both echocardiography (thickness) and MR images (area) in the same

cohort and found the epicardial fat depots to be smaller than paracardial fat, regardless of the imaging method applied (Sicari et al. 2011). We conclude that both fat depots are volatile in size within the general population and contribute with our results to the broader picture.

We found a median of 8.7 cm^2 for epicardial fat and 18.3 cm^2 for paracardial fat for all subjects (Rado et al. 2019) in the systolic assessment and 7.7 cm^2 and 16 cm^2 in the diastolic assessment, respectively. While every individual had measurable paracardial fat, the absence of measurable epicardial fat was noted in a few cases. We did not multiply the amount of fat with the slice thickness but worked with the primary numbers to avoid calculative bias. In a study conducted in Italy, MRI data derived from diastolic measurements showed a mean epicardial fat area of 8.27 cm^2 and mean paracardial fat area of 18.13 cm^2 (Sicari et al. 2011). Similar amounts have been reported by others (Sironi et al. 2012) and these data reflect our findings very well. We found that our results of epicardial fat are higher than for example by *Oyama et al* (Oyama et al. 2011) who measured epicardial fat areas in CT on certain anatomical levels in Japan. It is known that epicardial fat is ethnicity-dependent and therefore cannot be directly compared (Salami et al. 2013, Adams et al. 2017).

In general, men had higher median amounts of all fat depots than women, regardless of the systolic or diastolic measurements. Gender differences in epicardial fat have been described previously, e.g. by *Dagvasumberel et al*, who found higher epicardial fat volume in men as compared to women but differences became comparable when adjusting for height and body surface index (Dagvasumberel et al. 2012). *De Larochiellère et al* also found higher amounts of epicardial fat in men than in women (De Larochellière et al. 2014). However, it needs to be noted that our results are purely descriptive and have not been adjusted for height, weight or body surface area.

There was a strong correlation seen between data-sets derived from segmentations conducted in the maximal systole and the maximal diastole. Single-slice segmentation of pericardial fat depots in MRI in the long axis has been conducted in a couple of studies (Sironi et al. 2012, Sicari et al. 2011, Jonker et al. 2013, Van Schinkel et al. 2014) but to our knowledge, there are no cohort study data on the comparability of the diastolic and

systolic measurements in this view so far. *Teme et al* showed strong correlations between epicardial fat assessment in the end-systole and end-diastole on short-axis MR images in 20 subjects (Teme et al. 2014) and we support the same finding for the cardiac long-axis four chamber view in a cohort comprising 372 individuals. The highest correlation coefficient was seen for pericardial fat, followed by paracardial fat and then epicardial fat. We hypothesize that this finding relates to the absolute sizes of the fat depots. The strong correlations between both data sets also support the use of one dataset only for more sophisticated statistical analyses. It needs to be considered that the maximal systole and maximal diastole were determined subjectively on each image, which may theoretically constitute a source of error.

Data derived from the systolic measurements were generally larger for all fat depots as compared to measurements in the diastole. This finding may be explained by employing a single-slice measurement and the contraction of the heart during the systole drawing surrounding structures including the fat depots into the field of view. Similar observations have been made for echocardiographically derived epicardial fat thickness in systole and diastole (Graeff et al. 2016). As the epicardial fat depot is anatomically closer to the movements of the heart than the paracardial fat depot, differences between systole and diastole were slightly larger for the epicardial fat depot than for paracardial fat.

We found a significant increase in both the epicardial and paracardial fat depots from subjects with normal glucose tolerance to prediabetics and diabetics (Rado et al. 2019). Previous research found, that epicardial fat is increased in diabetes (Song et al. 2015) and even prediabetes (Arpaci et al. 2015). Moreover, epicardial fat thickness has been shown to be associated with diabetes prevalence in a male Korean cohort independent of multiple cardiovascular risk factors (Chun et al. 2015). *Iacobellis and Leonetti* stated, that there is a relation between epicardial fat and insulin-resistance (Iacobellis and Leonetti 2005). Thereby, our results are in line with the current literature and indicate that there may be structural changes in the body fat composition in impaired glucose metabolism and

insulin-resistance and the amount of epicardial fat seems to be associated with metabolic alterations.

However, there is not much literature on the increase of paracardial fat in the light of impaired glucose metabolism. *Thanassoulis et al* argued that paracardial fat is correlated with metabolic risk in a study comprising 3,312 participants (Thanassoulis et al. 2010a) and *Sicari et al* also found correlations between paracardial fat and signs for metabolic syndrome in a study cohort of 49 subjects (Sicari et al. 2011).

Data trends are very similar for assessment in the maximal diastole in the same study population. They also show a significant stepwise increase from healthy subjects to prediabetics and diabetics for both fat depots. However, and as discussed earlier, the absolute numbers are slightly smaller.

Upon adjustment for age and gender, the association between prediabetes and epicardial fat attenuated. Furthermore, in subjects with diabetes, a loss of significance was found after adjusting for age, gender and traditional cardiovascular risk factors, whereas the association of paracardial fat and diabetes remained significant after adjusting for age, gender, traditional cardiovascular risk factors, BMI and SAT. The association between paracardial fat and diabetes became only non-significant after the additional adjustment for VAT (Rado et al. 2019). The differences in the loss of significance between the prediabetes and diabetes group may be explained by the more advanced structural changes in diabetes as compared to prediabetes in the development of the disease. Interestingly, traditional cardiovascular risk factors can be depicted as confounders for the association between diabetes and epicardial fat in our study. High levels of interaction between different cardiovascular risk factors are known; it has, for example, been shown that epicardial fat is associated to smoking (Monti et al. 2014) and the metabolic syndrome (Wang et al. 2009). On the other hand, epicardial fat, smoking, diabetes, or age influence coronary artery disease (Jeong et al. 2007). In short, our results contradict previously conducted studies such as *Wang et al* who found independent associations between CT-measured epicardial fat and diabetic status (Wang et al. 2009).

Available data in the literature are scarce for paracardial fat. Interestingly, we detected an association of paracardial fat to diabetes even after adjusting for age, gender and traditional risk factors (Rado et al. 2019). This finding is interesting by showing that the fat depot distant to the myocardium is not primarily affected by typical cardiovascular risk factors. As has been described earlier, *Sicari et al* found that paracardial fat correlates better with cardiometabolic risk markers than epicardial fat (Sicari et al. 2011). However, all associations became non-significant after additional adjustment for VAT, thereby underlining the potency and uniqueness of this distinct fat depot as previously described in the Framingham Heart Study (Fox et al. 2007). We conclude from our data that there is no independent association between either epicardial or paracardial fat and impaired glucose metabolism (Rado et al. 2019). Nonetheless, our study analyzes the contributions of epicardial and paracardial fat towards impaired glucose metabolism and in the context of other cardiovascular risk factors in this stepwise approach in great detail.

In multivariate analysis, the strongest predictor for both epicardial and paracardial fat was VAT (Rado et al. 2019). Our results of this analysis are in line with other groups who reported a significant correlation particularly for epicardial fat and VAT (Iacobellis et al. 2003), and a correlation especially in obese diabetics (Jain et al. 2015). VAT has been discussed as one of the ectopic fat storage sites to be used when other fat storage sites cannot compensate anymore (Smith 2015). Our study underlines the importance of VAT in the development of cardiometabolic disease states due to its detrimental effects via epicardial adipose tissue. Earlier studies have even suggested epicardial fat as a measure for VAT (Iacobellis et al. 2003). Interestingly, *Graeff et al* analyzed epicardial fat thickness by echocardiography in the ELSA-Brasil study and found that associations to cardiometabolic variables were mostly influenced by age, gender, race and central adiposity which was measured as waist circumference in this particular study (Graeff et al. 2016).

A weaker association was found between epicardial fat and current smoking. As has been described, an association between epicardial fat and smoking has been discussed earlier in subjects with metabolic syndrome (Monti et al. 2014) and our study certainly comprises subjects with that complex metabolic manifestation.

It is known that paracardial fat correlates with VAT, as has been shown in the Framingham Heart Study by *Thanassoulis et al* (Thanassoulis et al. 2010a) and we are in line with that finding. Moreover, *Sironi et al* stated that it may be paracardial fat that is more associated with cardiovascular risk (Sironi et al. 2012), thus making it unclear to which extent which pericardial fat depot contributes to cardiovascular disease. Paracardial fat has been described to show an indifferent behavior between subcutaneous and epicardial fat as shown in the context of weight loss by *Foppa et al* (Foppa et al. 2013).

As our original cohort only comprises subjects without clinically manifest cardiovascular disease, we defined imaging-based parameters that represent subclinical pathological LV changes. The presence of LGE is a marker for focal fibrosis, for example after myocardial ischemia (Wu et al. 2001). LVCI is a marker for cardiac remodeling (Pun et al. 2011). An LVEF <55% has been suggested as a cutoff for patients with heart failure with preserved ejection fraction who may progress to reduced ejection fraction (Ueda et al. 2015). Interestingly, when combining these markers of LV impairment, both the epicardial and paracardial fat depots were higher in subjects fulfilling the criteria for this composite endpoint (Rado et al. 2019). Epicardial fat has been shown to affect the coronary microvasculature (Gaborit et al. 2012) and our findings also hint at a pathological influence of epicardial fat in the very early stages of LV impairment. Again, our study underlines the potential of imaging-based prevention in the future as very early LV changes can be detected before a clinical manifestation occurs.

When stepwise adjusted, the association between epicardial fat and the composite endpoint of LV impairment remained significant after adjustment for diabetes and other cardiovascular risk factors. Even upon additional adjustment for VAT, the association remained independent. However, when adjusted for BMI instead of VAT, the association was rendered non-significant (Rado et al. 2019). We currently do not have a sufficient explanation for this finding although our hypothesis is that the different fat depots that are summarized in the calculated BMI may play different roles in the human body (Rado et al. 2019). As described earlier, the epicardial fat depot is very close to the myocardium and the coronary vessels and they are not separated by a fascia (Corradi et al. 2004). Our

finding may emphasize the strong local effect that epicardial fat has on its surrounding structures, even in clinically cardiovascular healthy subjects (Rado et al. 2019).

Interestingly, the association between paracardial fat and LV impairment was rendered non-significant after adjusting for traditional cardiovascular risk factors including diabetes status (Rado et al. 2019). This finding may be explained by the anatomical remoteness of the paracardial fat depot to the myocardium and the coronary vessels.

Future Directions for the use of epicardial fat data as derived from MRI are promising. Firstly, due to its non-ionizing nature, MRI is a unique tool for screening clinically healthy subjects. Nowadays, the SSFP sequence is a standard sequence in most CMR protocols (Kramer et al. 2013), thereby not prolonging the measurement process or delaying the routine work-flow. The segmentation of the pericardial fat depots can easily be integrated into the reporting routine. Nevertheless, concerns about the financial aspects and length of performing CMR have been raised (Madonna et al. 2019). MRI-based screening for epicardial fat as a predictor for dysfunctional adiposity can, in the future, hopefully be offered to subjects with symptoms of the metabolic syndrome who are at risk for developing adverse cardiac events in the future. Also, subclinical LV impairment can be analyzed on these MR images before it becomes clinically manifest. Hopefully epi- and paracardial fat can be used as predictors for the overall fat status of an individual as well. BMI and waist circumference measurements could then be underpinned by more sophisticated fat analysis without subjects undergoing time-consuming whole-body MRIs. The planimetric assessment of cardiac fat could also be integrated in the workflow when performing necessary non-contrast calcium-scoring CTs. The assessment of epi- and paracardial fat should be seen as an integral part in analyzing the complete body structure and the creation of imaging-based panels related to clinical and laboratory measurements should be aspired. This could help determine the subject's overall metabolic status and improve the individual risk assessment. Additionally, these data could – with the individual's informed consent – then be applied to develop a plan for individualized prevention, diagnostics and therapies but also to calculate estimated healthcare costs not only or the individual but for the general population. Data can also

be used to compare them to a larger set of anthropometric measurements and other fat compartments in the human body, such as renal/retroperitoneal fat in order to fully understand the fat deposition in the human body.

The paracardial fat depot is widely unexamined and may very well not directly play a role in the development of cardiovascular disease but interact with the other different fat depots of the human body. Therefore, further research into this particular fat depot should be of high interest.

Our study has limitations. Firstly, our cohort consists of Caucasian Western-European subjects only, therefore results concerning the amount of pericardial fat compartments of our study are only partially applicable to other, ethnically more diverse populations as has been discussed previously (Rado et al. 2019) and shown in several studies conducted so far (Adams et al. 2017, Apfaltrer et al. 2014). Moreover, subjects in the three subgroups 'normal glucose tolerance', 'prediabetes' and 'diabetes' were not matched for e.g. age, gender or BMI and differed additionally in sample size. Thus, a part of our data has only descriptive character. We tried to overcome that fact by multivariate analysis but noted, that further prospective studies including matched and randomized subjects would be preferable (Rado et al. 2019). Also, subjects with prior cardiovascular disease were excluded from the study, thereby leaving the study cohort with clinically cardiovascular healthy subjects. In order to still analyze the effect of the fat depots on the left ventricle we had to employ imaging-based variables that helped us understand the subclinical implications of especially epicardial fat. Moreover, we could not analyze clinically manifest cardiac diseases and outcomes (Rado et al. 2019). While the previous facts may be seen as a limitation, it needs to be noted though, that this study is a baseline study and outcomes are not yet available. Thus, a longitudinal approach would be preferable in order to examine whether our findings with subclinical variables are of clinical significance in the future. Additionally, further studies including greater numbers of subjects with and without prior cardiovascular disease are warranted. Subjects included in the study were mostly not newly diagnosed with diabetes or under antidiabetic therapy according to German guidelines. This fact, together with the intake of cardioprotective medication in many study subjects, may have influenced our findings and may be

responsible for the early loss of significance concerning established cardiovascular risk factors. Also, we only included subjects with type 2 diabetes into the study. We segmented the pericardial fat depots manually. Also, maximal systole and diastole as well as the pericardium were subjectively identified, which may theoretically present a subjective source of error (Rado et al. 2019). Hence, a consensus reading was conducted to rule out possible great errors. Our study also shows a good correlation between manually and automatically assessed pericardial fat and we may hopefully overcome the problem of manual segmentation soon.

In conclusion, the manual assessment of the pericardial fat compartments on MR images in the cine SSFP-sequence in the long axis (four chamber view) is feasible with the chosen approach (Rado et al. 2019). There were strong correlations seen between data derived from the systole and the diastole while measurements from the systole were larger. Our manually derived data for pericardial fat from single-slice long-axis measurements correlated well with automatically derived, volumetric data for pericardial fat.

In all subjects included, the median paracardial fat depot was larger than the epicardial fat depot (Rado et al. 2019) and men had more median paracardial and epicardial fat than women. There were significant differences in epicardial as well as paracardial fat between healthy subjects, prediabetics and diabetics in our cohort without clinical manifest cardiovascular disease. However, the association between epicardial and paracardial fat to impaired glucose metabolism was not independent of other traditional cardiovascular risk factors. VAT was the strongest predictor for epicardial as well as paracardial fat in multivariate analysis (Rado et al. 2019). We also found an increase in subclinical measures of LV impairment ranging from healthy subjects to prediabetics and diabetics. Subjects with the composite endpoint of LV impairment had significantly higher amounts of both epicardial and paracardial fat. Upon stepwise adjustment, epicardial fat was independently associated with the composite endpoint of LV impairment, even when additionally adjusting for VAT but not for BMI. However, no independent association between paracardial fat and signs of subclinical LV impairment was found (Rado et al. 2019).

Our study contributes to a better scientific understanding of both the epicardial and paracardial fat depot. We underline the feasibility of manually analyzing the cardiac fat depots on a standard MRI sequence which opens new venues for image interpretation in the diagnostic routine. While there is no independent association between impaired glucose metabolism and epicardial or paracardial fat, our study emphasizes the importance of VAT in the development of cardiometabolic diseases and the local deteriorating effect that epicardial fat has on the myocardium independent of VAT. Finally, our study results indicate, that an increase of epicardial fat seems to be one of many factors within the complex pathomechanism of cardiovascular and metabolic alterations, even in subclinical diseases.

Abstract

Objective: To manually assess the pericardial fat depots on MRI (Magnetic Resonance Imaging) in a clinically cardiovascular healthy cohort and investigate associations between epicardial/paracardial fat and disturbances in the glucose metabolism as well as measures for subclinical left ventricular (LV) impairment.

Material and Methods: 400 subjects from the KORA FF4 cohort with established glucose tolerance status underwent whole-body 3 Tesla MRI exams. Segmentation of the pericardial fat depots in the systolic and diastolic heart cycle was performed manually using a cine steady-state free precession (SSFP) sequence in the four-chamber view. Late gadolinium enhancement, LV concentricity index > 1.3g/ml and LV ejection fraction <55% were used to define LV impairment.

Results: A total of 372 subjects were included in the final analysis. Systolic and diastolic measurements correlated very well (all $r \geq 0.90$). Epicardial and paracardial fat showed an increase from healthy subjects to prediabetics and diabetics (all $p<0.001$). The association between epicardial fat and diabetes became non-significant after adjusting for age, gender, hypertension, smoking, low-density lipoprotein (LDL) and triglycerides while paracardial fat remained significantly associated with diabetes even after additional adjustment for BMI and subcutaneous adipose tissue but not visceral adipose tissue (VAT). In multivariate analysis, VAT was the strongest predictor for epicardial and paracardial fat (both $p<0.001$). Epicardial fat was associated with subclinical measures of LV impairment independent of age, gender, smoking, diabetes status, hypertension, LDL and VAT ($p=0.02$) but not BMI ($p=0.09$).

Conclusion: Increased epicardial and paracardial fat seen in prediabetics and diabetics is not independent of other cardiovascular risk factors including VAT. Epicardial but not paracardial fat is associated with early signs for LV impairment.

Zusammenfassung

Ziel: Ziel der Arbeit war die manuelle Quantifizierung der perikardialen Fettdepots mittels MRT (Magentresonanztomographie) in einer klinisch kardiovaskulär gesunden Kohorte sowie die Bestimmung der Assoziation zwischen epikardialem/parakardialem Fett und gestörtem Glukosestoffwechsel sowie Zeichen subklinischer linksventrikulärer (LV) Einschränkung.

Material und Methoden: 400 Probanden aus der KORA FF4 Kohorte mit etabliertem Glukosetoleranzstatus wurden mittels 3 Tesla Ganzkörper MRT untersucht. Die Segmentierung der perikardialen Fettdepots im systolischen und diastolischen Herzzyklus erfolgte manuell unter Benutzung einer cine steady-state free precession (SSFP) Sequenz im Vierkammerblick. Late Gadolinium Enhancement, LV Konzentrizitätsindex >1.3g/ml und eine LV Ejektionsfraktion <55% wurden zur Definition der LV Einschränkung verwendet.

Ergebnisse: Es wurden 372 Probanden in die Analyse eingeschlossen. Systolische und diastolische Messungen korrelierten sehr gut (alle $r \geq 0.90$). Epikardiales und parakardiales Fett zeigten einen Anstieg von gesunden Probanden zu Prädiabetikern und Diabetikern (alle $p<0.001$). Die Assoziation zwischen epikardialem Fett und Diabetes wurde nicht signifikant nach Adjustierung für Alter, Geschlecht, Bluthochdruck, Rauchen, low-density lipoprotein (LDL) und Triglyceride. Parakardiales Fett blieb signifikant mit Diabetes auch nach zusätzlicher Adjustierung für BMI und subkutanes Fettgewebe aber nicht viszerales Fettgewebe (VAT) assoziiert. In der multivariaten Analyse war VAT der stärkste Prädiktor für epikardiales und parakardiales Fett (beide $p<0.001$). Epikardiales Fett war mit subklinischen Markern einer LV Schädigung unabhängig von Alter, Geschlecht, Rauchen, diabetischem Status, Bluthochdruck, LDL und VAT ($p=0.02$), aber nicht BMI ($p=0.09$) assoziiert.

Fazit: Erhöhtes epikardiales und parakardiales Fett bei Prädiabetikern und Diabetikern ist nicht unabhängig von anderen kardiovaskulären Risikofaktoren inklusive VAT. Epikardiales aber nicht parakardiales Fett ist mit frühen Zeichen einer LV Einschränkung assoziiert.

References

Adams DB, Narayan O, Munnur RK, Cameron JD, Wong DT, Talman AH, Harper RW, Seneviratne SK, Meredith IT and Ko BS (2017) Ethnic differences in coronary plaque and epicardial fat volume quantified using computed tomography. Int J Cardiovasc Imaging 33(2)**:** 241-249.

Adler AI, Boyko EJ, Ahroni JH, Stensel V, Forsberg RC and Smith DG (1997) Risk factors for diabetic peripheral sensory neuropathy. Results of the Seattle Prospective Diabetic Foot Study. Diabetes Care 20(7)**:** 1162-1167.

Alexopoulos N, McLean DS, Janik M, Arepalli CD, Stillman AE and Raggi, P (2010) Epicardial adipose tissue and coronary artery plaque characteristics. Atherosclerosis 210(1)**:** 150-154.

Ali S, Stone MA, Peters JL, Davies MJ and Khunti K (2006) The prevalence of co-morbid depression in adults with Type 2 diabetes: a systematic review and meta-analysis. Diabet Med 23(11)**:** 1165-1173.

Altin C, Sade LE, Gezmis E, Ozen N, Duzceker O, Bozbas H, Eroglu S and Muderrisoglu H (2016) Assessment of Subclinical Atherosclerosis by Carotid Intima-Media Thickness and Epicardial Adipose Tissue Thickness in Prediabetes. Angiology 67(10)**:** 961-969.

Altin C, Sade LE, Gezmis E, Yilmaz M, Ozen N and Muderrisoglu H (2017) Assessment of epicardial adipose tissue and carotid/femoral intima media thickness in insulin resistance. J Cardiol 69(6)**:** 843-850.

American Diabetes Association (2007) Standards of medical care in diabetes--2007. Diabetes Care 30(Suppl 1)**:** S4-S41.

American Diabetes Association (2010) Diagnosis and classification of diabetes mellitus. Diabetes Care 33(Suppl 1)**:** S62-S69.

American Diabetes Association (2014) Diagnosis and classification of diabetes mellitus. Diabetes Care 37(Suppl 1)**:** S81-S90.

American Diabetes Association (2018) 2. Classification and Diagnosis of Diabetes: Standards of Medical Care in Diabetes—2018. Diabetes Care 41(Suppl 1)**:** S13-S27.

Apfaltrer P, Schindler A, Schoepf UJ, Nance JW Jr., Tricarico F, Ebersberger U, Mcquiston AD, Meyer M, Henzler T, Schoenberg SO, Bamberg F and Vliegenthart R (2014) Comparison of epicardial fat volume by computed tomography in black versus white patients with acute chest pain. Am J Cardiol 113(3)**:** 422-428.

Arora RC, Waldmann M, Hopkins DA and Armour JA (2003) Porcine intrinsic cardiac ganglia. Anat Rec A Discov Mol Cell Evol Biol 271(1)**:** 249-258.

Arpaci D, Ugurlu BP, Aslan AN, Ersoy R, Akcay M and Cakir B (2015) Epicardial fat thickness in patients with prediabetes and correlation with other cardiovascular risk markers. Intern Med 54(9)**:** 1009-1014.

Arroyo C, Hu FB, Ryan LM, Kawachi I, Colditz GA, Speizer FE and Manson J (2004) Depressive symptoms and risk of type 2 diabetes in women. Diabetes Care 27(1)**:** 129-133.

Baig A, Campbell B, Russell M, Singh J and Borra S (2012) Epicardial fat necrosis: an uncommon etiology of chest pain. Cardiol J 19(4)**:** 424-428.

Baldasseroni S, Pratesi A, Orso F, Di Serio C, Foschini A, Marella AG, Bartoli N, Di Bari M, Fumagalli S, Marchionni N and Tarantini F (2013) Epicardial adipose tissue and insulin resistance in patients with coronary artery disease with or without left ventricular dysfunction. Monaldi Arch Chest Dis 80(4)**:** 170-176.

Bambace C, Telesca M, Zoico E, Sepe A, Olioso D, Rossi A, Corzato F, Di Francesco V, Mazzucco A, Santini F and Zamboni M (2011) Adiponectin gene expression and adipocyte diameter: a comparison between epicardial and subcutaneous adipose tissue in men. Cardiovasc Pathol 20(5)**:** e153-e156.

Bambace C, Sepe A, Zoico E, Telesca M, Olioso D, Venturi S, Rossi A, Corzato F, Faccioli S, Cominacini L, Santini F and Zamboni M (2014) Inflammatory profile in subcutaneous and epicardial adipose tissue in men with and without diabetes. Heart Vessels 29(1)**:** 42-48.

Bamberg F, Kauczor HU, Weckbach S, Schlett CL, Forsting M, Ladd SC, Greiser KH, Weber MA, Schulz-Menger J, Niendorf T, Pischon T, Caspers S, Amunts K, Berger K, Bülow R, Hosten N, Hegenscheid K, Kröncke T, Linseisen J, Günther M, Hirsch JG, Köhn A, Hendel T, Wichmann HE, Schmidt B, Jöckel KH, Hoffmann W, Kaaks R, Reiser MF, Völzke H for the German National Cohort MRI Study Investigators (2015) Whole-Body MR Imaging in the German National Cohort: Rationale, Design, and Technical Background. Radiology 277(1)**:** 206-220.

Bamberg F, Hetterich H, Rospleszcz S, Lorbeer R, Auweter SD, Schlett CL, Schafnitzel A, Bayerl C, Schindler A, Saam T, Müller-Peltzer K, Sommer W, Zitzelsberger T, Machann J, Ingrisch M, Selder S, Rathmann W, Heier M, Linkohr B, Meisinger C, Weber C, Ertl-Wagner B, Massberg S, Reiser MF and Peters A (2017) Subclinical Disease Burden as Assessed by Whole-Body MRI in Subjects With Prediabetes, Subjects With Diabetes, and Normal Control Subjects From the General Population: The KORA-MRI Study. Diabetes 66(1)**:** 158-169.

Bentata Y, Chemlal A, Karimi I, El Alaoui F, Haddiya I and Abouqal R (2015) Diabetic kidney disease and vascular comorbidities in patients with type 2 diabetes mellitus in a developing country. Saudi J Kidney Dis Transpl 26(5)**:** 1035-1043.

Bertaso AG, Bertol D, Duncan BB and Foppa M (2013) Epicardial fat: definition, measurements and systematic review of main outcomes. Arq Bras Cardiol 101(1)**:** e18-28.

Bommer C, Heesemann E, Sagalova V, Manne-Goehler J, Atun R, Barnighausen T and Vollmer S (2017) The global economic burden of diabetes in adults aged 20-79 years: a cost-of-illness study. Lancet Diabetes Endocrinol 5(6)**:** 423-430.

Britton KA and Fox CS (2011) Ectopic fat depots and cardiovascular disease. Circulation 124(24)**:** e837-841.

Burgeiro A, Fuhrmann A, Cherian S, Espinoza D, Jarak I, Carvalho RA, Loureiro M, Patrício M, Antunes M and Carvalho E (2016) Glucose uptake and lipid metabolism are impaired in epicardial adipose tissue from heart failure patients with or without diabetes. Am J Physiol Endocrinol Metab 310(7)**:** E550-564.

Caro JJ, Ward AJ and O'Brien JA (2002) Lifetime costs of complications resulting from type 2 diabetes in the U.S. Diabetes Care 25(3)**:** 476-481.

Cetin M, Cakici M, Polat M, Suner A, Zencir C and Ardic I (2013) Relation of epicardial fat thickness with carotid intima-media thickness in patients with type 2 diabetes mellitus. Int J Endocrinol 2013**:** 769175.

Chen O, Sharma A, Ahmad I, Bourji N, Nestoiter K, Hua P, Hua B, Ivanov A, Yossef J, Klem I, Briggs WM, Sacchi TJ and Heitner JF (2015) Correlation between pericardial, mediastinal, and intrathoracic fat volumes with the presence and severity of coronary artery disease, metabolic syndrome, and cardiac risk factors. Eur Heart J Cardiovasc Imaging 16(1)**:** 37-46.

Chen S, Anderson MV, Cheng WK and Wongworawat MD (2009) Diabetes associated with increased surgical site infections in spinal arthrodesis. Clin Orthop Relat Res 467(7)**:** 1670-1673.

Cheng VY, Dey D, Tamarappoo B, Nakazato R, Gransar H, Miranda-Peats R, Ramesh A, Wong ND, Shaw LJ, Slomka PJ and Berman DS (2010) Pericardial fat burden on ECG-gated noncontrast CT in asymptomatic patients who subsequently experience adverse cardiovascular events. JACC Cardiovasc Imaging 3(4)**:** 352-360.

Chun H, Suh E, Byun AR, Park HR and Shim KW (2015) Epicardial fat thickness is associated to type 2 diabetes mellitus in Korean men: a cross-sectional study. Cardiovasc Diabetol 14**:** 46.

Corradi D, Maestri R, Callegari S, Pastori P, Goldoni M, Luong TV and Bordi C (2004) The ventricular epicardial fat is related to the myocardial mass in normal, ischemic and hypertrophic hearts. Cardiovasc Pathol 13(6)**:** 313-316.

Dabbah S, Komarov H, Marmor A and Assy N (2014) Epicardial fat, rather than pericardial fat, is independently associated with diastolic filling in subjects without apparent heart disease. Nutr Metab Cardiovasc Dis 24(8)**:** 877-882.

Dagvasumberel M, Shimabukuro M, Nishiuchi T, Ueno J, Takao S, Fukuda D, Hirata Y, Kurobe H, Soeki T, Iwase T, Kusunose K, Niki T, Yamaguchi K, Taketani Y, Yagi S, Tomita N, Yamada H, Wakatsuki T, Harada M, Kitagawa T and Sata M (2012) Gender disparities in the association between epicardial adipose tissue volume and coronary atherosclerosis: a 3-dimensional cardiac computed tomography imaging study in Japanese subjects. Cardiovasc Diabetol 11**:** 106.

Davidovich D, Gastaldelli A and Sicari R (2013) Imaging cardiac fat. Eur Heart J Cardiovasc Imaging 14(7)**:** 625-630.

de Larochellière E, Coté J, Gilbert G, Bibeau K, Ross MK, Dion-Roy V, Pibarot P, Després JP and Larose E (2014) Visceral/epicardial adiposity in nonobese and apparently healthy young adults: association with the cardiometabolic profile. Atherosclerosis 234(1)**:** 23-29.

Deary IJ, Hepburn DA, MacLeod KM and Frier BM (1993) Partitioning the symptoms of hypoglycaemia using multi-sample confirmatory factor analysis. Diabetologia 36(8)**:** 771-777.

Devereux RB, Roman MJ, Paranicas M, O'Grady MJ, Lee ET, Welty TK, Fabsitz RR, Robbins D, Rhoades ER and Howard BV (2000) Impact of diabetes on cardiac structure and function: the strong heart study. Circulation 101(19)**:** 2271-2276.

Ding X, Terzopoulos D, Diaz-Zamudio M, Berman DS, Slomka PJ and Dey D (2015) Automated pericardium delineation and epicardial fat volume quantification from noncontrast CT. Med Phys 42(9)**:** 5015-5026.

Evin M, Broadhouse KM, Callaghan FM, McGrath RT, Glastras S, Kozor R, Hocking SL, Lamy J, Redheuil A, Kachenoura N, Fulcher GR, Figtree GA and Grieve SM (2016) Impact of obesity and epicardial fat on early left atrial dysfunction assessed by cardiac MRI strain analysis. Cardiovasc Diabetol 15(1)**:** 164.

Farrell C and Moran J (2014) Comparison of comorbidities in patients with pre-diabetes to those with diabetes mellitus type 2. Ir Med J 107(3)**:** 72-74.

Flüchter S, Haghi D, Dinter D, Heberlein W, Kühl HP, Neff W, Sueselbeck T, Borggrefe M and Papavassiliu T (2007) Volumetric assessment of epicardial adipose tissue with cardiovascular magnetic resonance imaging. Obesity (Silver Spring) 15(4)**:** 870-878.

Fong DS, Aiello LP, Ferris FL 3rd and Klein R (2004) Diabetic retinopathy. Diabetes Care 27(10)**:** 2540-2553.

Foppa M, Pond KK, Jones DB, Schneider B, Kissinger KV and Manning WJ (2013) Subcutaneous fat thickness, but not epicardial fat thickness, parallels weight reduction three months after bariatric surgery: a cardiac magnetic resonance study. Int J Cardiol 168(4)**:** 4532-4533.

Fowler MJ (2008) Microvascular and Macrovascular Complications of Diabetes. Clinical Diabetes 26(2)**:** 77-82.

Fox CS, Massaro JM, Hoffmann U, Pou KM, Maurovich-Horvat P, Liu CY, Vasan RS, Murabito JM, Meigs JB, Cupples LA, D'Agostino RB Sr. and O'Donnell CJ (2007) Abdominal visceral and subcutaneous adipose tissue compartments: association with metabolic risk factors in the Framingham Heart Study. Circulation 116(1)**:** 39-48.

Fukuda T, Bouchi R, Takeuchi T, Nakano Y, Murakami M, Minami I, Izumiyama H, Hashimoto K, Yoshimoto T and Ogawa Y (2018) Ratio of visceral-to-subcutaneous fat area predicts cardiovascular events in patients with type 2 diabetes. J Diabetes Investig 9(2)**:** 396-402.

Gaasch WH and Zile MR (2011) Left ventricular structural remodeling in health and disease: with special emphasis on volume, mass, and geometry. J Am Coll Cardiol 58(17)**:** 1733-1740.

Gaborit B, Kober F, Jacquier A, Moro PJ, Flavian A, Quilici J, Cuisset T, Simeoni U, Cozzone P, Alessi MC, Clément K, Bernard M and Dutour A (2012) Epicardial fat volume is associated with coronary microvascular response in healthy subjects: a pilot study. Obesity (Silver Spring) 20(6)**:** 1200-1205.

Gatidis S, Heber SD, Storz C and Bamberg F (2017) Population-based imaging biobanks as source of big data. Radiol Med 122(6)**:** 430-436.

Genuth S, Alberti KG, Bennett P, Buse J, Defronzo R, Kahn R, Kitzmiller J, Knowler WC, Lebovitz H, Lernmark A, Nathan D, Palmer J, Rizza R, Saudek C, Shaw J, Steffes M, Stern M, Tuomilehto J, Zimmet P and Expert Committee on the Diagnosis and Classification of Diabetes Mellitus (2003) Follow-up report on the diagnosis of diabetes mellitus. Diabetes Care 26(11)**:** 3160-3167.

Golan R, Shelef I, Rudich A, Gepner Y, Shemesh E, Chassidim Y, Harman-Boehm I, Henkin Y, Schwarzfuchs D, Ben Avraham S, Witkow S, Liberty IF, Tangi-Rosental O, Sarusi B, Stampfer MJ and Shai I (2012) Abdominal superficial subcutaneous fat: a putative distinct protective fat subdepot in type 2 diabetes. Diabetes Care 35(3)**:** 640-647.

Gorter PM, van Lindert AS, de Vos AM, Meijs MF, van der Graaf Y, Doevendans PA, Prokop M and Visseren FL (2008) Quantification of epicardial and peri-coronary fat using cardiac computed tomography; reproducibility and relation with obesity and metabolic syndrome in patients suspected of coronary artery disease. Atherosclerosis 197(2)**:** 896-903.

Graeff DB, Foppa M, Pires JC, Vigo A, Schmidt MI, Lotufo PA, Mill JG and Duncan BB (2016) Epicardial fat thickness: distribution and association with diabetes mellitus, hypertension and the metabolic syndrome in the ELSA-Brasil study. Int J Cardiovasc Imaging 32(4)**:** 563-572.

Grimaldi A, Grangé V, Allannic H, Passa P, Rodier M, Cornet P, Duprat I, Duc-Dodon P, Lemaire A, Liard F and Eschwège E (2000) Epidemiological analysis of patients with Type 2 diabetes in France. J Diabetes Complications 14(5)**:** 242-249.

Grundy SM, Brewer HB Jr., Cleeman JI, Smith SC Jr., Lenfant C, American Heart Association, National Heart Lung and Blood Institute (2004) Definition of metabolic syndrome: Report of the National Heart, Lung, and Blood Institute/American Heart Association conference on scientific issues related to definition. Circulation 109(3)**:** 433-438.

Hayashi T, Boyko EJ, Leonetti DL, McNeely MJ, Newell-Morris L, Kahn SE and Fujimoto WY (2003) Visceral adiposity and the risk of impaired glucose tolerance: a prospective study among Japanese Americans. Diabetes Care 26(3)**:** 650-655.

Heidemann C, Du Y, Paprott R, Haftenberger M, Rathmann W and Scheidt-Nave C (2016) Temporal changes in the prevalence of diagnosed diabetes, undiagnosed diabetes and prediabetes: findings from the German Health Interview and Examination Surveys in 1997-1999 and 2008-2011. Diabet Med 33(10)**:** 1406-1414.

Hetterich H, Bayerl C, Peters A, Heier M, Linkohr B, Meisinger C, Auweter S, Kannengießer SA, Kramer H, Ertl-Wagner B and Bamberg F (2016) Feasibility of a three-step magnetic resonance imaging approach for the assessment of hepatic steatosis in an asymptomatic study population. Eur Radiol 26(6)**:** 1895-1904.

Holle R, Happich M, Löwel H, Wichmann HE for the MONICA KORA Study Group (2005) KORA-a research platform for population based health research. Gesundheitswesen 67 Suppl 1**:** S19-S25.

Homsi R, Sprinkart AM, Gieseke J, Meier-Schroers M, Yuecel S, Fischer S, Nadal J, Dabir D, Luetkens JA, Kuetting DL, Schild HH and Thomas DK (2018) Cardiac magnetic resonance based evaluation of aortic stiffness and epicardial fat volume in patients with hypertension, diabetes mellitus, and myocardial infarction. Acta Radiol 59(1)**:** 65-71.

Iacobellis G, Assael F, Ribaudo MC, Zappaterreno A, Alessi G, Di Mario U and Leonetti F (2003) Epicardial fat from echocardiography: a new method for visceral adipose tissue prediction. Obes Res 11(2)**:** 304-310.

Iacobellis G and Leonetti F (2005) Epicardial adipose tissue and insulin resistance in obese subjects. J Clin Endocrinol Metab 90(11)**:** 6300-6302.

Iacobellis G, Barbaro G and Gerstein HC (2008a) Relationship of epicardial fat thickness and fasting glucose. Int J Cardiol 128(3)**:** 424-426.

Iacobellis G, Willens HJ, Barbaro G and Sharma AM (2008b) Threshold values of high-risk echocardiographic epicardial fat thickness. Obesity (Silver Spring) 16(4)**:** 887-892.

Iacobellis G (2009a) Relation of epicardial fat thickness to right ventricular cavity size in obese subjects. Am J Cardiol 104(11)**:** 1601-1602.

Iacobellis G and Willens HJ (2009b) Echocardiographic epicardial fat: a review of research and clinical applications. J Am Soc Echocardiogr 22(12)**:** 1311-1319; quiz 1417-1418.

Iacobellis G, Lonn E, Lamy A, Singh N and Sharma AM (2011) Epicardial fat thickness and coronary artery disease correlate independently of obesity. Int J Cardiol 146(3)**:** 452-454.

Iacobellis G, Barbarini G, Letizia C and Barbaro G (2014a) Epicardial fat thickness and nonalcoholic fatty liver disease in obese subjects. Obesity (Silver Spring) 22(2)**:** 332-336.

Iacobellis G, Diaz S, Mendez A and Goldberg R (2014b) Increased epicardial fat and plasma leptin in type 1 diabetes independently of obesity. Nutr Metab Cardiovasc Dis 24(7)**:** 725-729.

Iacobellis G, Zaki MC, Garcia D and Willens HJ (2014c) Epicardial fat in atrial fibrillation and heart failure. Horm Metab Res 46(8)**:** 587-590.

Jain S, Mahadevaiah M and Shivanagappa M (2015) A Comparative Study of Epicardial Fat Thickness and its Association with Abdominal Visceral Fat Thickness in Obese and Nonobese Type 2 Diabetes Subjects. J Cardiovasc Echogr 25(4)**:** 103-107.

Janik M, Hartlage G, Alexopoulos N, Mirzoyev Z, McLean DS, Arepalli CD, Chen Z, Stillman AE and Raggi P (2010) Epicardial adipose tissue volume and coronary artery calcium to predict myocardial ischemia on positron emission tomography-computed tomography studies. J Nucl Cardiol 17(5)**:** 841-847.

Jeong JW, Jeong MH, Yun KH, Oh SK, Park EM, Kim YK, Rhee SJ, Lee EM, Lee J, Yoo NJ, Kim NH and Park JC (2007) Echocardiographic epicardial fat thickness and coronary artery disease. Circ J 71(4)**:** 536-539.

Jonker JT, de Mol P, de Vries ST, Widya RL, Hammer S, van Schinkel LD, van der Meer RW, Gans RO, Webb AG, Kan HE, de Koning EJ, Bilo HJ and Lamb HJ (2013) Exercise and type 2 diabetes mellitus: changes in tissue-specific fat distribution and cardiac function. Radiology 269(2)**:** 434-442.

Kannel WB and McGee DL (1979) Diabetes and cardiovascular disease. The Framingham study. JAMA 241(19)**:** 2035-2038.

Kaplan O, Kurtoglu E, Gozubuyuk G, Dogan C, Acar Z, Eyupkoca F and Pekdemir H (2015) Epicardial adipose tissue thickness in patients with chronic obstructive pulmonary disease having right ventricular systolic dysfunction. Eur Rev Med Pharmacol Sci 19(13)**:** 2461-2467.

Kaye SA, Folsom AR, Sprafka JM, Prineas RJ and Wallace RB (1991) Increased incidence of diabetes mellitus in relation to abdominal adiposity in older women. J Clin Epidemiol 44(3)**:** 329-334.

Kiraz K, Gökdeniz T, Kalaycioglu E, Börekci A, Akyol S, Baykan AO, Acele A, Karakoyun S, Seker T and Gür M (2016) Epicardial fat thickness is associated with severity of disease in patients with chronic obstructive pulmonary disease. Eur Rev Med Pharmacol Sci 20(21)**:** 4508-4515.

Kota SK, Meher LK, Jammula S, Kota SK and Modi KD (2012) Clinical profile of coexisting conditions in type 1 diabetes mellitus patients. Diabetes Metab Syndr 6(2)**:** 70-76.

Kramer CM, Barkhausen J, Flamm SD, Kim RJ, Nagel E and Society for Cardiovascular Magnetic Resonance Board of Trustees Task Force on Standardized Protocols

(2013) Standardized cardiovascular magnetic resonance (CMR) protocols 2013 update. J Cardiovasc Magn Reson 15**:** 91.

Lemieux S, Bédard A, Piché ME, Weisnagel SJ, Corneau L and Bergeron J (2011) Visceral adipose tissue accumulation and cardiovascular disease risk profile in postmenopausal women with impaired glucose tolerance or type 2 diabetes. Clin Endocrinol (Oxf) 74(3)**:** 340-345.

Levelt E, Pavlides M, Banerjee R, Mahmod M, Kelly C, Sellwood J, Ariga R, Thomas S, Francis J, Rodgers C, Clarke W, Sabharwal N, Antoniades C, Schneider J, Robson M, Clarke K, Karamitsos T, Rider O and Neubauer S (2016) Ectopic and Visceral Fat Deposition in Lean and Obese Patients With Type 2 Diabetes. J Am Coll Cardiol 68(1)**:** 53-63.

Ligthart S, van Herpt TT, Leening MJ, Kavousi M, Hofman A, Stricker BH, van Hoek M, Sijbrands EJ, Franco OH and Dehghan A (2016) Lifetime risk of developing impaired glucose metabolism and eventual progression from prediabetes to type 2 diabetes: a prospective cohort study. Lancet Diabetes Endocrinol 4(1)**:** 44-51.

Lin PJ, Kent DM, Winn A, Cohen JT and Neumann PJ (2015) Multiple chronic conditions in type 2 diabetes mellitus: prevalence and consequences. Am J Manag Care 21(1)**:** e23-34.

Liu J, Fox CS, Hickson DA, May WD, Hairston KG, Carr JJ and Taylor HA (2010) Impact of abdominal visceral and subcutaneous adipose tissue on cardiometabolic risk factors: the Jackson Heart Study. J Clin Endocrinol Metab 95(12)**:** 5419-5426.

Liu Y, Fu W, Lu M, Huai S, Song Y and Wei Y (2016) Role of miRNAs in Epicardial Adipose Tissue in CAD Patients with T2DM. Biomed Res Int 2016**:** 1629236.

Low S, Tai ES, Yeoh LY, Liu YL, Liu JJ, Tan KH, Fun S, Su C, Zhang X, Subramaniam T, Sum CF and Lim SC (2016) Onset and progression of kidney disease in type 2 diabetes among multi-ethnic Asian population. J Diabetes Complications 30(7)**:** 1248-1254.

Löwel H, Döring A, Schneider A, Heier M, Thorand B, Meisinger C for the MONICA KORA Study Group (2005) The MONICA Augsburg surveys--basis for prospective cohort studies. Gesundheitswesen 67 Suppl 1**:** S13-S18.

Machann J, Thamer C, Schnoedt B, Haap M, Haring HU, Claussen CD, Stumvoll M, Fritsche A and Schick F (2005) Standardized assessment of whole body adipose tissue topography by MRI. J Magn Reson Imaging 21(4)**:** 455-462.

Madonna R, Massaro M, Scoditti E, Pescetelli I and De Caterina R (2019) The epicardial adipose tissue and the coronary arteries: dangerous liaisons. Cardiovasc Res 115(6)**:** 1013-1025.

Mahabadi AA, Massaro JM, Rosito GA, Levy D, Murabito JM, Wolf PA, O'Donnell CJ, Fox CS and Hoffmann U (2009) Association of pericardial fat, intrathoracic fat, and visceral abdominal fat with cardiovascular disease burden: the Framingham Heart Study. Eur Heart J 30(7)**:** 850-856.

Mahabadi AA, Lehmann N, Kälsch H, Robens T, Bauer M, Dykun I, Budde T, Moebus S, Jöckel KH, Erbel R and Möhlenkamp S (2014) Association of epicardial adipose tissue with progression of coronary artery calcification is more pronounced in the early phase of atherosclerosis: results from the Heinz Nixdorf recall study. JACC Cardiovasc Imaging 7(9)**:** 909-916.

Marchington JM, Mattacks CA and Pond CM (1989) Adipose tissue in the mammalian heart and pericardium: structure, foetal development and biochemical properties. Comp Biochem Physiol B 94(2)**:** 225-232.

Marchington JM and Pond CM (1990) Site-specific properties of pericardial and epicardial adipose tissue: the effects of insulin and high-fat feeding on lipogenesis and the incorporation of fatty acids in vitro. Int J Obes 14(12)**:** 1013-1022.

Mazurek T, Zhang L, Zalewski A, Mannion JD, Diehl JT, Arafat H, Sarov-Blat L, O'Brien S, Keiper EA, Johnson AG, Martin J, Goldstein BJ and Shi Y (2003) Human epicardial adipose tissue is a source of inflammatory mediators. Circulation 108(20)**:** 2460-2466.

Melchior H, Kurch-Bek D and Mund M (2017) The Prevalence of Gestational Diabetes. Dtsch Arztebl Int 114(24)**:** 412-418.

Menke A, Casagrande S, Geiss L and Cowie CC (2015) Prevalence of and Trends in Diabetes Among Adults in the United States, 1988-2012. JAMA 314(10)**:** 1021-1029.

Mohammedi K, Woodward M, Marre M, Colagiuri S, Cooper M, Harrap S, Mancia G, Poulter N, Williams B, Zoungas S and Chalmers J (2017) Comparative effects of microvascular and macrovascular disease on the risk of major outcomes in patients with type 2 diabetes. Cardiovasc Diabetol 16(1)**:** 95.

Monti M, Monti A, Murdolo G, Di Renzi P, Pirro MR, Borgognoni F and Vincentelli GM (2014) Correlation between epicardial fat and cigarette smoking: CT imaging in patients with metabolic syndrome. Scand Cardiovasc J 48(5)**:** 317-322.

Neeland IJ, Turer AT, Ayers CR, Powell-Wiley TM, Vega GL, Farzaneh-Far R, Grundy SM, Khera A, McGuire DK and de Lemos JA (2012) Dysfunctional adiposity and the risk of prediabetes and type 2 diabetes in obese adults. JAMA 308(11)**:** 1150-1159.

Nelson AJ, Worthley MI, Psaltis PJ, Carbone A, Dundon BK, Duncan RF, Piantadosi C, Lau DH, Sanders P, Wittert GA and Worthley SG (2009) Validation of cardiovascular magnetic resonance assessment of pericardial adipose tissue volume. J Cardiovasc Magn Reson 11**:** 15.

Ogurtsova K, da Rocha Fernandes JD, Huang Y, Linnenkamp U, Guariguata L, Cho NH, Cavan D, Shaw JE and Makaroff LE (2017) IDF Diabetes Atlas: Global estimates for the prevalence of diabetes for 2015 and 2040. Diabetes Res Clin Pract 128**:** 40-50.

Oyama N, Goto D, Ito YM, Ishimori N, Mimura R, Furumoto T, Kato F, Tsutsui H, Tamaki N, Terae S and Shirato H (2011) Single-slice epicardial fat area measurement: do we need to measure the total epicardial fat volume? Jpn J Radiol 29(2)**:** 104-109.

Patterson CC, Dahlquist GG, Gyürüs E, Green A, Soltész G and the EURODIAB Study Group (2009) Incidence trends for childhood type 1 diabetes in Europe during 1989-2003 and predicted new cases 2005-20: a multicentre prospective registration study. Lancet 373(9680)**:** 2027-2033.

Petersen SE, Matthews PM, Francis JM, Robson MD, Zemrak F, Boubertakh R, Young AA, Hudson S, Weale P, Garratt S, Collins R, Piechnik S and Neubauer S (2016) UK Biobank's cardiovascular magnetic resonance protocol. J Cardiovasc Magn Reson 18**:** 8.

Pun SC, Figura M, Chow K, Haykowsky M, Thompson R and Paterson I (2011) A simple method for characterizing left ventricular remodeling by cardiovascular magnetic resonance. J Cardiovasc Magn Reson 13(Suppl 1)**:** P277.

Rado SD, Lorbeer R, Gatidis S, Machann J, Storz C, Nikolaou K, Rathmann W, Hoffmann U, Peters A, Bamberg F and Schlett CL (2019) MRI-based assessment and characterization of epicardial and paracardial fat depots in the context of impaired glucose metabolism and subclinical left-ventricular alterations. Br J Radiol 92(1096)**:** 20180562.

Rodriguez-Monforte M, Sánchez E, Barrio F, Costa B and Flores-Mateo G (2017) Metabolic syndrome and dietary patterns: a systematic review and meta-analysis of observational studies. Eur J Nutr 56(3)**:** 925-947.

Rosito GA, Massaro JM, Hoffmann U, Ruberg FL, Mahabadi AA, Vasan RS, O'Donnell CJ and Fox CS (2008) Pericardial fat, visceral abdominal fat, cardiovascular disease risk factors, and vascular calcification in a community-based sample: the Framingham Heart Study. Circulation 117(5)**:** 605-613.

Rutter MK, Parise H, Benjamin EJ, Levy D, Larson MG, Meigs JB, Nesto RW, Wilson PW and Vasan RS (2003) Impact of glucose intolerance and insulin resistance on cardiac structure and function: sex-related differences in the Framingham Heart Study. Circulation 107(3)**:** 448-454.

Sacks HS and Fain JN (2007) Human epicardial adipose tissue: a review. Am Heart J 153(6)**:** 907-917.

Sacks HS, Fain JN, Holman B, Cheema P, Chary A, Parks F, Karas J, Optican R, Bahouth SW, Garrett E, Wolf RY, Carter RA, Robbins T, Wolford D and Samaha J (2009) Uncoupling protein-1 and related messenger ribonucleic acids in human epicardial and other adipose tissues: epicardial fat functioning as brown fat. J Clin Endocrinol Metab 94(9)**:** 3611-3615.

Salami SS, Tucciarone M, Bess R, Kolluru A, Szpunar S, Rosman H and Cohen G (2013) Race and epicardial fat: the impact of anthropometric measurements, percent body fat and sex. Ethn Dis 23(3)**:** 281-285.

Sarin S, Wenger C, Marwaha A, Qureshi A, Go BD, Woomert CA, Clark K, Nassef LA and Shirani J (2008) Clinical significance of epicardial fat measured using cardiac multislice computed tomography. Am J Cardiol 102(6)**:** 767-771.

Schlett CL, Lorbeer R, Arndt C, Auweter S, Machann J, Hetterich H, Linkohr B, Rathmann W, Peters A and Bamberg F (2018) Association between abdominal adiposity and subclinical measures of left-ventricular remodeling in diabetics, prediabetics and normal controls without history of cardiovascular disease as measured by magnetic resonance imaging: results from the KORA-FF4 Study. Cardiovasc Diabetol 17(1)**:** 88.

Schram MT, Henry RM, van Dijk RA, Kostense PJ, Dekker JM, Nijpels G, Heine RJ, Bouter LM, Westerhof N and Stehouwer CD (2004) Increased central artery stiffness in impaired glucose metabolism and type 2 diabetes: the Hoorn Study. Hypertension 43(2)**:** 176-181.

Seissler J, Feghelm N, Then C, Meisinger C, Herder C, Koenig W, Peters A, Roden M, Lechner A, Kowall B and Rathmann W (2012) Vasoregulatory peptides pro-endothelin-1 and pro-adrenomedullin are associated with metabolic syndrome in the population-based KORA F4 study. Eur J Endocrinol 167(6)**:** 847-853.

Seppälä T, Saxen U, Kautiainen H, Järvenpää S and Korhonen PE (2013) Impaired glucose metabolism and health related quality of life. Prim Care Diabetes 7(3)**:** 223-227.

Sequeira DI, Ebert LC, Flach PM, Ruder TD, Thali MJ and Ampanozi G (2015) The correlation of epicardial adipose tissue on postmortem CT with coronary artery stenosis as determined by autopsy. Forensic Sci Med Pathol 11(2)**:** 186-192.

Sicari R, Sironi AM, Petz R, Frassi F, Chubuchny V, De Marchi D, Positano V, Lombardi M, Picano E and Gastaldelli A (2011) Pericardial rather than epicardial fat is a cardiometabolic risk marker: an MRI vs echo study. J Am Soc Echocardiogr 24(10)**:** 1156-1162.

Sironi AM, Petz R, De Marchi D, Buzzigoli E, Ciociaro D, Positano V, Lombardi M, Ferrannini E and Gastaldelli A (2012) Impact of increased visceral and cardiac fat on cardiometabolic risk and disease. Diabet Med 29(5)**:** 622-627.

Smith U (2015) Abdominal obesity: a marker of ectopic fat accumulation. J Clin Invest 125(5)**:** 1790-1792.

Song DK, Hong YS, Lee H, Oh JY, Sung YA and Kim Y (2015) Increased Epicardial Adipose Tissue Thickness in Type 2 Diabetes Mellitus and Obesity. Diabetes Metab J 39(5)**:** 405-413.

Starup-Linde J, Frost M, Vestergaard P and Abrahamsen B (2017) Epidemiology of Fractures in Diabetes. Calcif Tissue Int 100(2)**:** 109-121.

Stöckl D, Rückert-Eheberg IM, Heier M, Peters A, Schipf S, Krabbe C, Völzke H, Tamayo T, Rathmann W and Meisinger C (2016) Regional Variability of Lifestyle Factors and Hypertension with Prediabetes and Newly Diagnosed Type 2 Diabetes Mellitus: The Population-Based KORA-F4 and SHIP-TREND Studies in Germany. PLoS One 11(6)**:** e0156736.

Storz C, Heber SD, Rospleszcz S, Machann J, Sellner S, Nikolaou K, Lorbeer R, Gatidis S, Elser S, Peters A, Schlett CL and Bamberg F (2018) The role of visceral and subcutaneous adipose tissue measurements and their ratio by magnetic resonance imaging in subjects with prediabetes, diabetes and healthy controls from a general population without cardiovascular disease. Br J Radiol 91(1089)**:** 20170808.

Swifka J, Weiss J, Addicks K, Eckel J and Rösen P (2008) Epicardial fat from guinea pig: a model to study the paracrine network of interactions between epicardial fat and myocardium? Cardiovasc Drugs Ther 22(2)**:** 107-114.

Tamayo T, Brinks R, Hoyer A, Kuß OS and Rathmann W (2016) The Prevalence and Incidence of Diabetes in Germany. Dtsch Arztebl Int 113(11)**:** 177-182.

Teijeira-Fernandez E, Eiras S, Grigorian-Shamagian L, Fernandez A, Adrio B and Gonzalez-Juanatey JR (2008) Epicardial adipose tissue expression of adiponectin is lower in patients with hypertension. J Hum Hypertens 22(12)**:** 856-863.

Teme T, Sayegh B, Syed M, Wilber D, Bakhos L and Rabbat M (2014) Quantification of epicardial fat volume using cardiovascular magnetic resonance imaging. J Cardiovasc Magn Reson 16 (Suppl 1)**:** O112.

Thanassoulis G, Massaro JM, Hoffmann U, Mahabadi AA, Vasan RS, O'Donnell CJ and Fox CS (2010a) Prevalence, distribution, and risk factor correlates of high pericardial and intrathoracic fat depots in the Framingham heart study. Circ Cardiovasc Imaging 3(5)**:** 559-566.

Thanassoulis G, Massaro JM, O'Donnell CJ, Hoffmann U, Levy D, Ellinor PT, Wang TJ, Schnabel RB, Vasan RS, Fox CS and Benjamin EJ (2010b) Pericardial fat is

associated with prevalent atrial fibrillation: the Framingham Heart Study. Circ Arrhythm Electrophysiol 3(4)**:** 345-350.

Ueda T, Kawakami R, Nishida T, Onoue K, Soeda T, Okayama S, Takeda Y, Watanabe M, Kawata H, Uemura S and Saito Y (2015) Left Ventricular Ejection Fraction (EF) of 55% as Cutoff for Late Transition From Heart Failure (HF) With Preserved EF to HF With Mildly Reduced EF. Circ J 79(10)**:** 2209-2215.

van Schinkel LD, Sleddering MA, Lips MA, Jonker JT, de Roos A, Lamb HJ, Jazet IM, Pijl H and Smit JW (2014) Effects of bariatric surgery on pericardial ectopic fat depositions and cardiovascular function. Clin Endocrinol (Oxf) 81(5)**:** 689-695.

Vasques AC, Souza JR, Yamanaka A, De Oliveira Mda S, Novaes FS, Pareja JC and Geloneze B (2013) Sagittal abdominal diameter as a marker for epicardial adipose tissue in premenopausal women. Metabolism 62(7)**:** 1032-1036.

Venteclef N, Guglielmi V, Balse E, Gaborit B, Cotillard A, Atassi F, Amour J, Leprince P, Dutour A, Clément K and Hatem SN (2015) Human epicardial adipose tissue induces fibrosis of the atrial myocardium through the secretion of adipo-fibrokines. Eur Heart J 36(13)**:** 795-805a.

Vural M, Talu A, Sahin D, Elalmis OU, Durmaz HA, Uyanik S and Dolek BA (2014) Evaluation of the relationship between epicardial fat volume and left ventricular diastolic dysfunction. Jpn J Radiol 32(6)**:** 331-339.

Wang CP, Hsu HL, Hung WC, Yu TH, Chen YH, Chiu CA, Lu LF, Chung FM, Shin SJ and Lee YJ (2009) Increased epicardial adipose tissue (EAT) volume in type 2 diabetes mellitus and association with metabolic syndrome and severity of coronary atherosclerosis. Clin Endocrinol (Oxf) 70(6)**:** 876-882.

Wang ZJ, Reddy GP, Gotway MB, Yeh BM, Hetts SW and Higgins CB (2003) CT and MR imaging of pericardial disease. Radiographics 23 Spec No**:** S167-180.

Westerberg DP (2013) Diabetic ketoacidosis: evaluation and treatment. Am Fam Physician 87(5)**:** 337-346.

World Health Organization and International Diabetes Federation (2006) Definition and diagnosis of diabetes mellitus and intermediate hyperglycemia: report of a WHO/IDF consultation [online]. World Health Organization, Geneva, Switzerland.
URL:https://www.who.int/diabetes/publications/Definition%20and%20diagnosis%20of%20diabetes_new.pdf [Zugriff 13.05.2019]

Wu E, Judd RM, Vargas JD, Klocke FJ, Bonow RO and Kim RJ (2001) Visualisation of presence, location, and transmural extent of healed Q-wave and non-Q-wave myocardial infarction. Lancet 357(9249)**:** 21-28.

Wu FZ, Huang YL, Wu CC, Wang YC, Pan HJ, Huang CK, Yeh LR and Wu MT (2016) Differential Effects of Bariatric Surgery Versus Exercise on Excessive Visceral Fat Deposits. Medicine (Baltimore) 95(5)**:** e2616.

Wu J, Ward E, Threatt T and Lu ZK (2017) Progression to Type 2 Diabetes and Its Effect on Health Care Costs in Low-Income and Insured Patients with Prediabetes: A Retrospective Study Using Medicaid Claims Data. J Manag Care Spec Pharm 23(3)**:** 309-316.

Würslin C, Machann J, Rempp H, Claussen C, Yang B and Schick F (2010) Topography mapping of whole body adipose tissue using A fully automated and standardized procedure. J Magn Reson Imaging 31(2)**:** 430-439.

Xu G, Liu B, Sun Y, Du Y, Snetselaar LG, Hu FB and Bao W (2018) Prevalence of diagnosed type 1 and type 2 diabetes among US adults in 2016 and 2017: population based study. BMJ 362**:** k1497.

Xu WL, Qiu CX, Wahlin A, Winblad B and Fratiglioni L (2004) Diabetes mellitus and risk of dementia in the Kungsholmen project: a 6-year follow-up study. Neurology 63(7)**:** 1181-1186.

Yau JW, Rogers SL, Kawasaki R, Lamoureux EL, Kowalski JW, Bek T, Chen SJ, Dekker JM, Fletcher A, Grauslund J, Haffner S, Hamman RF, Ikram MK, Kayama T, Klein BE, Klein R, Krishnaiah S, Mayurasakorn K, O'Hare JP, Orchard TJ, Porta M, Rema M, Roy MS, Sharma T, Shaw J, Taylor H, Tielsch JM, Varma R, Wang JJ, Wang N, West S, Xu L, Yasuda M, Zhang X, Mitchell P, Wong TY for the Meta-Analysis for Eye Disease (META-EYE) Study Group (2012) Global prevalence and major risk factors of diabetic retinopathy. Diabetes Care 35(3)**:** 556-564.

Yerramasu A, Dey D, Venuraju S, Anand DV, Atwal S, Corder R, Berman DS and Lahiri A (2012) Increased volume of epicardial fat is an independent risk factor for accelerated progression of sub-clinical coronary atherosclerosis. Atherosclerosis 220(1)**:** 223-230.

Yudkin JS, Eringa E and Stehouwer CD (2005) "Vasocrine" signalling from perivascular fat: a mechanism linking insulin resistance to vascular disease. Lancet 365(9473)**:** 1817-1820.

Erklärung zum Eigenanteil

Die Arbeit wurde am Universitätsklinikum Tübingen in der Abteilung für Diagnostische und Interventionelle Radiologie unter der Betreuung von Prof. Dr. Fabian Bamberg durchgeführt.

Die KORA (Kooperative Gesundheitsforschung in der Region Augsburg) Studie wird vom Helmholtz Zentrum München geleitet. Die Konzeption der hier vorliegenden Analyse erfolgte durch Prof. Dr. Bamberg, PD Dr. Sergios Gatidis und mich, Sophia D. Rado.

Die Auswertung der Bilder (manuelle Segmentation von epi- und perikardialem Fett in Systole und Diastole) wurde durch mich, Sophia D. Rado, durchgeführt und ich habe auch die Intrareader Daten erhoben. PD. Dr. Sergios Gatidis erhob die Interreader Daten und wir haben zusammen das Konsensus-reading durchgeführt.
Weitere MRT-basierte Daten (automatisiert erhobenes perikardiales Fettvolumen, Herzfunktionsparameter, VAT, SAT, $PDFF_{hepatic}$) sowie klinische Kovariablen, die für die statistische Auswertung benötigt wurden, waren im Vorhinein im Rahmen der allgemeinen KORA Studienauswertung erhoben worden und standen in der Datenbank bereit.

Die statistische Auswertung erfolgte durch Dr. rer. med. Roberto Lorbeer, Mitarbeiter des Instituts für klinische Radiologie der Ludwig-Maximilians-Universität München, im Rahmen der Datenauswertung für die geplante wissenschaftliche Publikation als Teil der KORA-Studie nach Entwicklung des Analysekonzepts durch mich, Sophia D. Rado, und mit Anregungen von PD. Dr. Christopher L. Schlett. Die Tabellen wurden alle von mir entworfen, teils mit Anregungen von PD. Dr. Christopher L. Schlett. Graphiken 1 und 3 habe ich selbstständig erstellt, Graphik 2 wurde dankenswerterweise von KORA-Studienkoordination, Institut für Epidemiologie II, Helmholtz Zentrum München zur Verfügung gestellt. Material für die Graphiken 4 und 5 wurden dankenswerterweise von PD. Dr. Jürgen Machann, Tübingen, zur Verfügung gestellt. Die restlichen Graphiken

wurden von Dr. Roberto Lorbeer im Rahmen der wissenschaftlichen Analyse nach Vorschlägen meinerseits, erstellt.

Die aus den Daten hervorgegangene wissenschaftliche Publikation habe ich selbständig mit Korrekturen und Anregungen durch PD. Dr. Christopher L. Schlett verfasst.

Die Literaturrecherche für die hier vorliegende Arbeit habe ich selbstständig durchgeführt.

Ich versichere, das hier vorliegende Manuskript selbständig verfasst zu haben (Korrekturen und Anregungen durch Prof. Dr. Fabian Bamberg, PD. Dr. Christopher L. Schlett und Dr. rer. med. Roberto Lorbeer) und keine weiteren als die von mir angegebenen Quellen verwendet zu haben.

Mainz, den 05.07.2019

Sophia D. Rado

List of publications

Parts of this work have been previously published in the following publication:

Rado, SD, Lorbeer, R, Gatidis, S, Machann, J, Storz, C, Nikolaou, K, Rathmann, W, Hoffmann, U, Peters, A, Bamberg, F and Schlett, CL (2019) MRI-based assessment and characterization of epicardial and paracardial fat depots in the context of impaired glucose metabolism and subclinical left-ventricular alterations. Br J Radiol 92**:** 20180562.

Acknowledgements

I thank my doctoral supervisor, Prof. Dr. Fabian Bamberg, for his support during this project. Dr. rer. med. Roberto Lorbeer for his support in statistics and always being accessible for questions and comments. PD. Dr. Christopher L. Schlett for important remarks and support especially during the publication process. PD. Dr. Sergios Gatidis for his support during my training. The researchers that developed, initialized, organized, managed, performed and processed the KORA MRI project.

I thank my parents, Dr. Viktoria M. Heber and Dipl-Ing. Hans K. Heber, for their love and support. My husband Dr. Yaron Rado for always standing by my side and always encouraging me to aim higher. Drs. Corinna Storz and Sven Walter for our friendship.